GOLD

Growing energy crops on contaminated land for biofuels and soil remediation

D2.4

Process configurations, gas conditions and contamination content in gas and solid phase of entrained flow gasification and syngas cleaning

This project has received funding from the European Union's Horizon 2020 Research and Innovation Programme under Grant Agreement No. 101006873.

Document Summary

Deliverable Number: 2.4

Version: 1.0

Due date: 29.02.2024

Actual submission date: 27.02.2024

Work Package: WP2 - Conversion process for clean liquid biofuel production

Task: 2.1.3: Process and gas phase modelling & Task 2.3: Entrained flow gasification and gas cleaning

Lead beneficiary: TUM-CES

Editors/Authors: Marcel, Dossow; Sebastian, Fendt

Dissemination level: Public

Document history

Version	Date	Beneficiary	Author/Reviewer
1.0	27-02-2024	TUM-CES	Marcel, Dossow; Marlon, Ritz, Sebastian, Fendt; Anne, Oppelt

Horizon 2020 Grant Agreement Number: 101006873

Project Start Date: 15 April 2021

Duration: 48 months

Project coordinator: CRES

Partners

CRES - Centre for Renewable Energy Sources and Saving Foundation, Greece
AUA – Geoponiko Panepistimion Athinon, Greece
TUM - Technische Universität München, Germany
RE-CORD - Consorzio per la Ricerca e la Dimostrazione sulle Energie Rinnovabili, Italy
ETA - ETA Energia, Trasporti, Agricoltura, Italy
Uni-Lublin - Uniwersytet Marii Curie-Sklodowskiej, Poland
TNO - Nederlandse Organisatie Voor Toegepast Natuurwetenschappelijkonderzoek TNO, Netherlands
CERTH - ETHNIKO KENTRO EREVNAS KAI TECHNOLOGIKIS ANAPTYXIS, Greece
UNIBO - Alma Mater Studiorum - Università di Bologna, Italy
INRAE - Institut National de Recherche pour l'Agriculture, l'Alimentation et l'Environnement, France
YNCREA HDF – Junia, France
UNL - Universidade Nova de Lisboa, Portugal
ICL - Imperial College of Science Technology and Medicine, United Kingdom
WR - Stichting Wageningen Research, Netherlands
METE S.A. - METE AE METALLEFTIKI EMPORIKI TEHNIKI AE*MINING TRADING TECHNICAL SA, Greece
IITD - Indian Institute of Technology Delhi, India
HUNAN - Hunan Agricultural University, China
UDES - Université de Sherbrooke, Canada
IBFC - Institute of Bast Fiber Crops, Chinese Academy of Agricultural Sciences, China
CTD - Society for Economic and Social Studies, Center for Technology and

Executive Summary

The GOLD project's Biomass-to-Liquid process route 1 (WP2 – European Partners) offers a dual benefit of reclaiming contaminated land for agriculture while producing sustainable biofuels. Thermochemical conversion of pretreated biomass into syngas is achieved via high-temperature entrained flow gasification, with subsequent fermentation to ethanol and higher alcohols. Heavy metal contaminants are removed in the non-leachable slag. Syngas composition is crucial for fermentation, with the process requiring an O_2-free feed gas. A thermodynamic model is used to estimate industrial-scale syngas compositions. The process model by TUM-CES optimizes equipment interaction and overall design, increasing carbon efficiency to 40%. Thermodynamic modelling and experimental results validate the release behaviour of volatile heavy metals, with slightly higher volatilization temperatures observed in the BabiTER. ETV-ICP-OES is chosen as the standard method for measuring heavy metal release from contaminated biomass due to its versatility and productivity.

Table of contents

List of Tables

List of Figures

1. Introduction

The pollution of agricultural land is a great threat in Europe and globally. According to a study by the European Environment Agency (EAA), an estimated number of 2.5 million sites are contaminated in Europe, and 34.8% of the contamination is caused by heavy metals [Panagos etal. 2013]. Due to this problem, vast areas of land can't be used for food or animal feed production and the contaminants can be hazardous for all living organisms. Phytoremediation, using plants to remove, degrade, or stabilize contaminants in the soil, presents an inexpensive and environmentally beneficial and promising new approach to recover contaminated land for agricultural use. Due to long remediation times for heavy metals to be removed, phytoremediation on its own is not economically feasible unless the produced biomass can be valorised. [van Ginneken etal. 2007]

Biofuels, produced via biomass-to-liquid (BtL) processes as a sustainable, carbon-neutral alternative to conventional fuels, are often confronted with the direct or indirect competition with food production. Increased exploitation of biomass can lead to an increase of food and feed prices and to the creation of additional agricultural land, i.e., indirect land use change (ILUC). Thus, combining the two targets of recovering contaminated land for agricultural use while producing clean and sustainable biofuels with little indirect land use change (ILUC) from high-yield lignocellulosic plants, the GOLD project presents an economically and environmentally promising approach. Plants, which are optimized for phytoremediation purposes, are grown on and harvested from contaminated land (WP1). In the presented GOLD process route 1 as illustrated in Figure 1, the contaminated biomass is thermochemically converted into advanced biofuels (WP2). An effective conversion method for biomass-to-syngas is high-temperature entrained-flow gasification as investigated at the TUM Chair of Energy Systems (TUM-CES). After gas cleaning, the produced syngas can be fermented to ethanol and higher alcohols while heavy metals and metalloid contaminants are preferably removed in the non-leachable, vitrified slag.

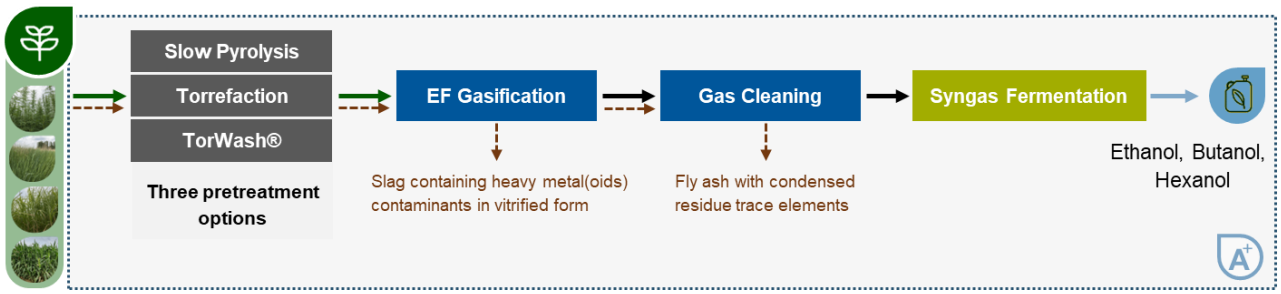

Figure 1: GOLD thermochemical conversion route 1 via biomass pretreatment, entrained flow gasification, gas cleaning and syngas fermentation to produce higher alcohols from contaminated soils.

Task 2.1.3: Process and gas phase modelling and Task 2.3: Entrained flow gasification and gas cleaning of the GOLD project investigate the WP2 process route 1 via entrained-flow gasification at high temperatures and moderate pressure and, after gas cleaning, the fermentation of the created synthesis gas in a bioreactor. The aim of this work is to predict and measure the fate of heavy metals and metalloids during gasification, determine syngas conditions and contamination after gasification and the resulting implications for gas cleaning before synthesis. For this purpose, TUM-CES investigates the fate of heavy metals from a process-level perspective employing both, experimental and simulative methods. FactSage modelling of the phase transition behaviour from solid to gas phase and electrothermal vaporization (ETV) coupled with inductively coupled plasma optical emission spectrometry (ICP-OES) is used for the temperature-resolved measurement of the release of heavy metals from biomass during gasification conditions. The phase transition of heavy metals and metalloids as well as gasification kinetics are also measured in lab-scale experiments using a wire mesh reactor (WMR) and the Baby High Temperature Entrained Flow Reactor (BabiTER).

2. Fundamentals, Material and Methods

TUM-CES activities in GOLD Task: 2.1.3: Process and gas phase modelling and Task 2.3: Entrained flow gasification and gas cleaning, follows two major objectives:

1. enabling syngas provision for syngas fermentation purposes in the required quality and purity while concentrating heavy metals in a vitrified, non-leachable form;
2. evaluate overall process performance (biomass-to-liquid system boundaries) to enable process scale-up and support GOLD WP3 activities.

To understand the implications on syngas composition when using heavily contaminated biomass in a gasification-based Biomass-to-Liquid (BtL) setup, first, the fundamentals of the main conversion steps from solid biomass to high-quality syngas are explained.

2.1. Principles of Gasification, Gas Cleaning and Syngas Fermentation

To produce syngas as the main intermediate in the thermochemical BtL process, the biomass feedstock is thermally decomposed through gasification taking place at high temperatures (1200–1800 °C). The gas mixture consisting of mainly CO, H_2, and CO_2, steam, potentially CH_4, and other minor trace substances, is then separated, conditioned, and cleaned to produce pure syngas. Gasification itself is divided in three steps. During drying the fuel is dried at approx. 100°C. Through this, the stored water within the fuel is vaporized. The degree of moisture of the used biomass has a significant effect on the energy efficiency of the whole process. On the other hand, the energy spends for drying the fuel to prevent later efficiency losses must also be accounted for, which respectively drops the energy efficiency of the whole process. In the following step of pyrolysis all volatile parts of the fuel are released. Volatile matter makes up the largest mass fraction of solid biomass. The volatile components form a burnable gas which may contain solid and fluid by-products such as tar compounds, oil and char. In the last step, the gasification, the remaining char and the by-products are brought to reaction with gasification agents like air, oxygen, CO_2 or steam to create a hydrogen and carbon monoxide rich gas.

Typical impurities in the syngas after gasification of biomass include solids (slag, char, ash), halide compounds, nitrogen and sulfur contaminants that can lead to erosion, corrosion, catalyst poisoning and deposits on downstream equipment. The downstream process steps determine syngas purity requirements. Possible syngas conditioning processes include quenching with a subsequent scrubber, (sour) water gas shift (WGS) and gas cleaning such as acid gas removal (AGR).

The gasification process is based on combining well-established technologies. as an advanced production route close to commercial operation, thus leveraging existing sugar and oil and gas industries infrastructure Gasification combined with a suitable biomass pretreatment technology not only enables high flexibility in feedstock acceptance, but also allows low development and demonstration costs for industry stakeholders through the decoupling of feedstock supply and feedstock conversion. Commercialization of biomass gasification as major conversion step is mainly hindered by high associated capital costs requiring economies of scale and high utilization, as well as technical challenges associated with the thermal, chemical, and material handling characteristics of biomass. Engineering for the successful implementation of Biomass-to-Syngas primarily should focus on adapting established technologies to the specific conditions and characteristics of the feedstock.

2.1.1. Produced Syngas Composition

Biomass gasification can be classified into allothermal gasification with heat supplied externally, and autothermal gasification in which the required heat is supplied by partial combustion of the fuel. The produced syngas at the outlet of the gasification reactor consists of different chemical components, which can be classified into desired and inert gases, as well as unwanted pollution due to impurities in the feedstock.

Desired gases are burnable and combustible to the lower heating value (LHV) of the derived syngas. Particularly important for the LHV are the H_2 and CO fractions. CH_4 also contributes but is only present in small amounts. Inert gases (e.g. N^2) are diluting the product gas and thus decreasing the LHV. The fractions of burnable and inert gas components are mainly influenced by the used gasification agent, temperature and mode of operation. Figure 2 gives an overview of possible variations of heat supply and gasification agents. Furthermore, different types of biomass are characterized by different compositions in regard of moisture, ash, and trace substances as well as different LHV. The impact of different biomass feedstocks on the composition of the syngas is, despite these differences, very low. On the contrary, impurities and pollution have a significant influence on the product gas.

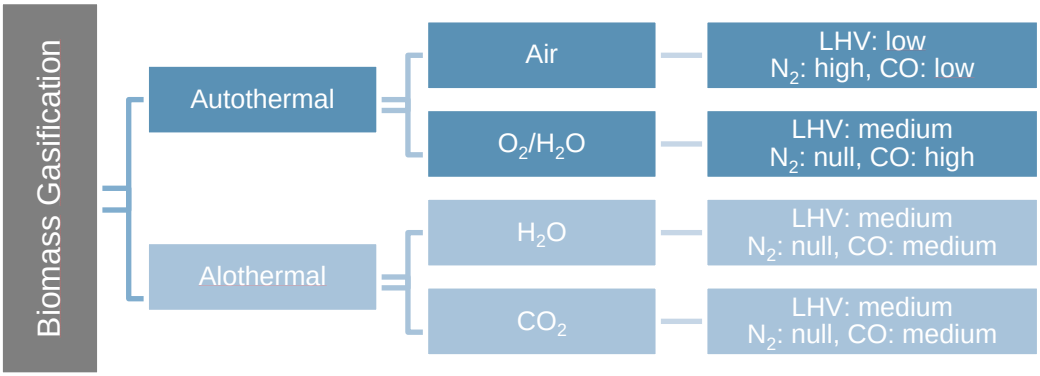

Figure 2: Comparison of gasification concepts and impact on syngas quality and composition [Kaltschmitt & Hartmann, 2009].

Allothermal gasification is typically operated with steam. The syngas produced has a LHV of about 10 MJ/m^3 and the set of problems due to tar fraction is mitigated. Autothermal gasification is normally operated with air or O_2 as gasification agent. If air is used, the product gas has a relatively low LHV of about 3 to 5 MJ/m^3, as the inert N^2 is not contributing to it. Depending on the reactor design, high fractions of tar can make the gas purification process complex. On the other hand, air is cheap and can be easily handled, which makes it a promising gasification agent for the use in small facilities. A variety of chemical reactions take part in the gasification process. The most important ones are show in Table 1. The required heat supply in autothermal gasification processes is primarily provided by the oxidation of carbon in the reactions 1 and 2. The Boudouard reaction (no.5) and the heterogeneous hydrogen reaction (no.6) have a significant impact on the product composition. The products (CO and H_2) fundamentally determine the heating value of the product gas.

The most characteristic feature of biomass gasification processes is the choice of reactor type, which has the largest impact on product gas composition and efficiency. In this work, slagging, oxygen-blown entrained flow gasification (EFG), is selected to produce the highest-quality syngas. In EFG a mixture of powdery biomass and gasification agents is injected into the reactor and immediately gasified at temperatures above 1200°C. The high temperatures lie above the ash melting point, such that fluid ash (slag) can be withdrawn from the reactor. High temperatures result in an increasing reaction rate of chemical reactions. Thus, for a constant residence time within the reactor, a faster approach to the equilibrium values of the chemical reaction can be achieved. On the other hand, equilibrium values of a reaction are also temperature dependent.

Table 1: Gasification reactions with heat of reaction [Higman & Van der Burgt, 2008].

Chemical Reactions		Δh	No.
C + O_2	⇔ CO_2	- 394 MJ/kmol	1
C + ½ O_2	⇔ CO	- 111 MJ/kmol	2
CO + ½ O_2	⇔ CO_2	- 283 MJ/kmol	3
H_2 + ½ O_2	⇔ H_2O	- 242 MJ/kmol	4
Boudard-reaction			
C + CO_2	⇔ 2 CO	+ 172 MJ/kmol	5
Heterogenous hydrogen reaction			
C + H_2O	⇔ CO + H_2	+ 131 MJ/kmol	6
Methanation			
C + 2 H_2	⇔ CH_4	- 75 MJ/kmol	7
Homogeneous hydrogen reactions			
CO + H_2O	⇔ CO_2 + H_2	- 41 MJ/kmol	8
Steam reforming			
CH_4 + H_2O	⇔ CO + 3 H_2	+ 206 MJ/kmol	9

Using pure O_2 as the gasification agent, high temperatures and high levels H_2/CO with a low CH_4 content and almost no tars present in the syngas can be reached. Table 2 exemplarily compares the syngas compositions from autothermal gasification using different gasification agents. The amount of O_2 provided to the gasification chamber is expressed via the molar ratio of the O_2 content to stoichiometric O_2 required (λ). In general, the gasification temperature increases with increasing λ. The pure O_2 needs to be supplied externally, e.g. via cryogenic air separation. In EFG, the minimum gasification temperature is limited by the gasification kinetics, ash properties and desired syngas composition. To avoid CH_4 formation, temperatures above 1400 °C are recommended. In EFG, the syngas composition, the H_2/CO ratio, can be adjusted within certain limits. The use of steam as additional gasification agent increases the syngas output and reduces CH_4 formation. Steam addition also favors the reduction of CO while promoting H_2 formation through WGS reaction. O_2 addition, on the other hand, results in an increased λ, lead to more combustion activity and reduces the H_2/CO ratio.

Table 2: Product gas composition and lower heating values (LHV) for authermal gasification processes [Kaltschmitt & Hartmann, 2009].

gas (in % vol)	Air	O_2 (EFG)
H_2	11 – 20	29 – 35
CO	12 – 19	35 – 44
CO_2	10 – 15	17 – 22
CH_4	2 – 5	< 1
N_2	45 – 60	3 – 9
LHV in MJ/m³	4 – 6	9 – 11

2.1.2. Syngas Impurities, Heavy Metal Release and Gas Cleaning

In fixed or fluidized bed gasification, pollutants within the product gas are mostly tar compounds from the devolatilization process, which could not split up due to too low temperatures and a too short residence time inside the gasification reactor. In EFG, tar components are decomposed in the gasification chamber and the syngas produced can be considered tar free. Besides, the product gas contains dust particles and, depending on the design of the reactor, different fractions of sulphur, halogen, heavy metals, and nitrogen compounds. All these impurities can cause erosion, corrosion, and deposits on downstream processes, especially the synthesis. In addition, the purity of the syngas is an economic challenge as high investment costs of gas purification must be offset by lower product yields and increased maintenance costs without gas purification.

Furthermore, secondary pollution is caused if heavy metals and metalloids are released or leached into the atmosphere during the gasification of contaminated biomass. The metals can neither be created nor destructed during gasification, but they change their phase and chemical form, and solid and gaseous heavy metal and metalloid compounds arise due to volatilization and condensation at different places of the reactor. Therefore, it is necessary to trap and separate the contaminants at some point in the process chain, preferably in a non-leachable, vitrified form.

According to Baxter (1993), metals are contained in biomass in two fractions. Most of the heavy metals are atomically dispersed and associated with oxygen-containing functional groups of the biomass, e.g as cations or chelates, and therefore incorporated in the biomass matrix. These metals are influenced both by their inherent volatility and by convective transport during the release of volatile biomass compounds. The second fraction is mostly added from extraneous sources during processing on the field, which causes them to be particulate and not associated with the biomass matrix. These metals are not influenced as strongly by the release of volatiles and undergo chemical reactions and phase changes determined by their thermochemical properties and interactions with the reaction atmosphere. [Baxter 1993, Linak and Wendt 1994]

It is expected that heavy metals and metalloids sublimate or react forming gaseous compounds in gasification processes [Obernberger etal. (1997), Vervaeke etal. 2006, Cui etal. 2018]. After the metals are initially vaporized at sufficient temperatures in the burner zone of the reactor, they form ultrafine aerosol particles by homogeneous nucleation or condense on existing particles or aerosols. In the cooler post-incineration zone of the reactor, the aerosols grow by heterogeneous coagulation, i.e. adhesion and agglomeration, on fly ash particles and only a small fraction stays in the syngas [Linak and Wendt 1993, Cui etal. 2018]. Thus, heavy metals and metalloids can either be enriched in the syngas, they can be enriched in the fly ash together with fine ash particles in the flue gas, or they can be enriched in the bottom ash/slag in the gasification chamber.

If heavy metals and metalloids were enriched in the syngas, downstream gas cleaning is necessary to remove these contaminants before the syngas is utilized or released into the environment. Techniques such as scrubbing, absorption, adsorption, or catalytic conversion can be employed to capture and remove the heavy metals and metalloids from the syngas stream (see below). As wastewater generated from the removal processes may contain concentrated levels of contaminants, proper treatment is essential to ensure compliance with environmental regulations before discharge or reuse. If heavy metals are enriched in the fly ash, specialized filtration and separation systems can be employed. Once collected, the fly ash can be treated to immobilize the contaminants or disposed of in a controlled manner. If heavy metals are enriched in the bottom ash or slag, they are immobilized in a non-leachable vitrified form, which facilitates their management and disposal. The vitrification process essentially locks the contaminants into the solid matrix, reducing the risk of leaching into the environment. As a result, disposal of bottom ash or slag enriched with heavy metals in non-leachable form is typically easier and safer compared to other forms of contamination making it the desired outcome in gasification processes. Regardless of the enrichment location, residues from downstream processes such as bottom ash, slag, fly ash, or captured contaminants need appropriate management, including storage, treatment, and disposal, to prevent environmental contamination.

In any case, gas cleaning after gasification is mandatory. Different purification steps are necessary depending on the desired application of the product gas. The required process configuration is determined by the downstream utilization of the product gas. All gas cleaning methods work at temperatures considerably lower than those of the EFG itself. Therefore, since there is always the need to cool the syngas, all entrained ash particles will inevitably pass through the critical temperature range where the ash becomes sticky. The best way to avoid this problem is to quench the gas as quickly as possible to a temperature at which the ash becomes solid, typically about 900 °C. Quenching is relatively reliable and inexpensive compared to cooling by

heat exchangers, but also less efficient because it degrades the thermal energy in the syngas to a medium-low temperature. For entrained flow slagging gasifiers, quenching can be accomplished using either a gas, chemical or water quench. Chemical quenching is used for multi-stage gasifiers. The hot gas leaving the first slagging stage of an EFG is used in the endothermic water gas reaction to gasify a second stage feed. Chemical quenching or quenching with gas is limited to temperatures of 900 °. Syngas coming from gasification can also be quenched by direct evaporation of water. When molten ash enters the water quenching area, the sudden drop in temperature causes it to solidify. The slag leaves the gasifier through a lock-hopper system at the bottom of the quench. The amount and quality of the slag depends on the used feedstock. It can be distinguished between partial quench, where only just enough water is evaporated to cool the gas to a specific temperature, and a total quench, in which sufficient water is evaporated to saturate the gas with water vapor. A full quench section serves also as a first gas treatment section to ensure safe and low maintenance operation.

To produce liquid fuel from syngas originating from biomass gasification processes, a synthesis-tailored gas cleaning is required to further reduce the concentration of pollutants. Thus, the downstream synthesis, i.e. syngas fermentation in the GOLD project, dictates the gas cleaning requirements. The choice of microorganism and its resilience to common syngas impurities are crucial considerations with significant implications for gas cleaning processes. Various inhibitory components present in syngas can significantly impact the syngas fermentation process. NH_3 can hinder the activity of hydrogenases and also H_2S is proven to inhibit enzymes. Additionally, NO has demonstrated inhibitory effects on hydrogenases, whereas NO_2 can hinder the function of formate dehydrogenase and nitrate reductase. Nitrate, serving as an alternative electron acceptor, has been observed to inhibit CO consumption. Nitrite, despite its potential utility as an electron acceptor for certain Clostridia strains, can also exhibit toxicity even at low concentrations. Notably, HCN stands out as a critical impurity in biogenic syngas due to its inhibitory and toxic effects. Other impurities like COS act as noncompetitive inhibitors for CO dehydrogenase. [Rückel et al., 2022] Table 3 shows the requirements for the synthesis gas for the investigated bacterium *C. carboxidivorans* in comparison to a catalytic synthesis process. The stated purity requirements are conservative estimates based on literature data, as these depend on depend on a variety of factors such as the reactor concept used. As can be seen, the purity requirements for gas fermentation are gas fermentation are not as demanding as those of catalytic synthesis.

Table 3: Provisional feed gas phase specifications for different contaminants and different synthesis pathways [Rückel el. al., 2021; Xu et al.., 2011; Arena, 2012].

Contamination	Gas fermentation (C. Carboxidivorans)	Catalytic synthesis
HCN	<10ppm	<10ppb
NH_3	Can be beneficial	<10ppb
NOx	<100ppm	<100ppb
Sulphur (H_2S)	<1000ppm	<100ppb
Halogens (HCl)	-	<10ppb
Particles	Very low concentration	Very low concentration
Tars	Very low concentration	Very low concentration

As mentioned above, chloride compounds might cause fouling, create deposits, and cause poisoning of (bio)catalysts while WGS and AGR units can experience problems related to ammonia. Depending on impurities in the raw syngas, cyclones, filters, or scrubbers can be used for particle separation. Cyclones can efficiently separate high particle loads and are therefore often used for the initial cleaning of the product gas stream. Scrubbers connected in series are used to remove remaining tars, particles, and most other water-soluble impurities (HCl, HCN, NH_3, and CO_2) by spraying the syngas with water. The water is collected at the bottom of the scrubber, is purified, and recycled. Syngas leaves the scrubber saturated.

If further purification of the product gas is necessary, absorption or adsorption processes can be used. Absorptive processes such as the amine process are only economically viable for large gas product streams and corresponding loads of impurities. With entrained flow gasification having almost no tar and particles in the produced syngas, and syngas fermentation limiting scale-up of the gasification system, an adsorption-based gas cleaning technology was chosen for the GOLD project.

Adsorption describes the binding of gas molecules to a solid with a porous surface, the adsorbent. Adsorption can be determined by three effects: Steric, kinetic and equilibrium effects. Adsorption is divided into chemisorption and physisorption. As a surface reaction, the maximum capacity of adsorption is proportional to the available surface area and porosity of the adsorbent. The most established adsorbent materials are metal oxides and activated carbon. The choice of adsorbent is determined by the impurities to be removed from the product gas. As tars, particles and NO_x do not pose a problem in EFG, the impurities relevant for this gas purification step before syngas fermentation are COS, H_2S, HCN, HCl, and heavy metals. H_2S can be separated with metal oxides such as Co, Cu, Fe, Mn, Mo, or Zn. The most common adsorbent for H_2S is ZnO. ZnO is also suitable for adsorptive HCl separation. The purification of HCN via chemisorption is still the subject of research and has not been commercialized. CuO and MgO are being investigated as possible adsorbents.

In this conditioning step, single gas components are withdrawn or certain ratios of wanted components are set. For example, the ratio of CO_2/CO can be set by using the catalysed water-gas-shift (WGS) reaction. Depending on the reaction temperature, H2 (forward WGS) or CO (reverse WGS) can be concentrated. Pressure swing adsorption (PSA) processes are considered the most suitable technology to remove H_2 or CO2 capture from hot syngas streams. PSA processes operating at elevated temperatures require upstream desulfurization processes as discussed above. In general, adsorbents used in high temperature PSA processes are not negatively affected by the presence of water, which is often used for the regeneration of the adsorption bed. PSA used for H_2 or CO2 recovery can achieve high purities (>95% CO_2 and >99% H_2) and high recovery rates (>90% CO_2 and >80% H_2) [Riboldi and Bolland 2017, Relvas et al., 2018].

2.2. Thermodynamic Phase Transition Model

Except for mercury (Hg), there is nearly no kinetic data on the behavior of trace elements during fuel conversion processes available in the literature. Therefore, global equilibrium analysis is often used as a first approach. In the GOLD project, a simulation model has been developed and validated based on global equilibrium analysis using FactSage, an integrated database computing system developed collaboratively by Thermfact/CRCT (Montreal, Canada) and GTT-Technologies (Aachen, Germany). Global equilibrium analysis is based on the minimization of the total Gibbs free energy of a system, while kinetics and local conditions are not considered. Global equilibrium analysis is based on the minimization of the total Gibbs free energy of a system while also considering the mass balance. A system is in thermodynamic equilibrium if the total Gibbs free energy is at a minimum. This means that every compound is in its thermodynamically most stable species and phase at the respective temperature and pressure and all reactions have reached equilibrium. In global equilibrium analysis, only global parameters (temperature, pressure, total composition) of the system are considered while local conditions, like temperature and pressure gradients in the burner zone, are neglected. The necessary thermodynamic data is generated by calculating the Gibbs free energy of a component at a given temperature.

The modelling framework developed by [Ritz etl al. 2023] is used to predict the phase transition behavior of heavy metals and metalloids from solid phase to gas phase in EFG and from gas phase to solid phase during full water quench and a schematic overview is provided in Figure 3. The modelling software FactSage provides several compound and solution databases containing model parameters for the calculation of the Gibbs free

energy of pure compounds and solutions as a function of temperature and composition. The databases used in this work are FactPS and GTOx (see Section 4.1.1). Gibbs free energy minimization is carried out in the FactSage module "Equilib", which requires the input of the temperature, pressure, and composition of the biomass, gasification agent, and carrier gas. The output is the concentration of the chemical species present at thermodynamic equilibrium at the given temperature and pressure.

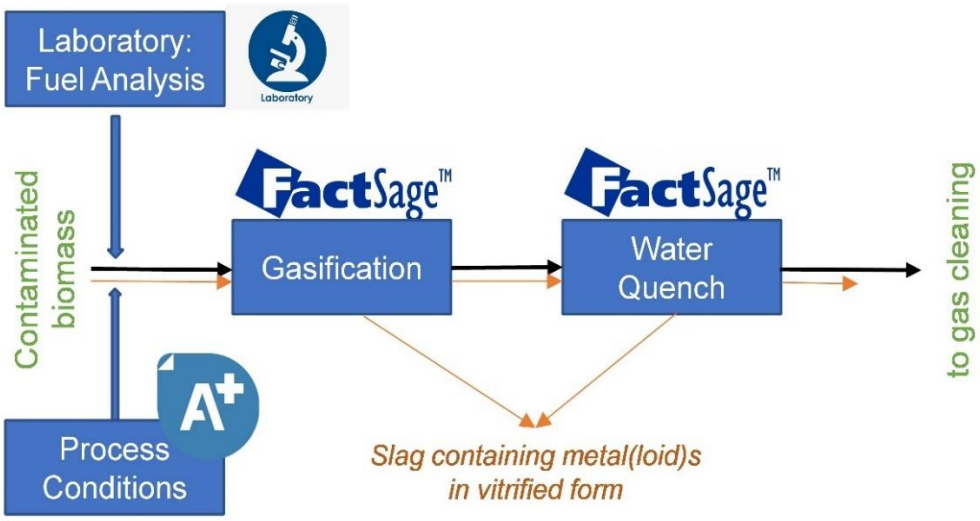

Figure 3: Schematics of the Thermodynamic Phase Transition Model in FactSage to determine the fate of heavy metals during gasification and quench. Black arrows: Biomass flow, orange arrows: contaminants, blue arrows: information input [Ritz etl al. 2023].

To simulate the release behaviour of the heavy metal metalloid contaminants in EFG using global equilibrium analysis in FactSage, the elemental composition of the biomass, which is obtained from fuel analysis, is directly used as input. The fuel analysis of the contaminated biomass as carried out by the TUM-CES includes the proximate analysis, the ultimate analysis, and the determination of LHV and HHV according to DIN 51900-1. The mass fraction of all metals, including heavy metals and metalloids, was measured by ICP-OES. In the proximate analysis, the moisture, ash, and volatiles content are measured, the fixed-C content is calculated. In the ultimate analysis, the mass fraction of C, H, N, S and Cl are determined. The mass fraction of oxygen is calculated by closing the mass balance, taking the inorganic fraction measured by ICP-OES into account. The remaining model input parameters are linked to the operating conditions. The temperature is varied from 900 °C to 2200 °C in steps of 100 °C. The equivalence ratio is chosen to be 0.34, which is typical for EFG. Thus, the corresponding temperature, 1800 °C, is the actual gasification temperature. The gasification agent used in this work is pure O_2. An Aspen Plus model is used to determine the respective equivalence ratio that is necessary to achieve a desired gasification temperature (see Section 2.3.4), taking into account the CO_2 employed as carrier gas at a loading of fuel per carrier gas rate of 300kg/m³. [Ritz etl al. 2023]

Simulating the EFG reaction chamber, all gas phase reactions are assumed to have reached equilibrium due to the high temperatures. When modelling the water quench, the assumption that all reactions have reached equilibrium cannot be made as the system is merely cooled down and species are not participating in further reactions. Therefore, the gas phase that is received from the modelling of the reaction chamber at gasification temperature (1800 °C) is used as input and the temperature is varied down from 1800 °C to 200 °C. Only the heavy metals and metalloids are included in an inert environment consisting of nitrogen (N) and an excess of quench water (H_2O), to prevent reactions. The concentration is taken from the mass of the heavy metals compared to the total mass of the gas phase and the phase transition behaviour in elemental form at the respective partial pressure is received.

2.3. Experimental Gasification Test Rigs at TUM used in GOLD WP2

2.3.1. Electrothermal Vaporization (ETV) and Inductively Coupled Plasma Optical Emission Spectrometry (ICP-OES)

The temperature-resolved release of heavy metals from biomass is measured in this work by electrothermal vaporization (ETV) coupled with inductively coupled plasma optical emission spectrometry (ICP-OES). For this purpose, a SPECTR*O* ARCO*S 2* ICP-OES spectrometer from SPECTRO Analytical Instruments GmbH, Germany, and an ET*V* 4000 from Spectral Systems GmbH, Germany, equipped with the AD-50 autosampler, are used.

Calibration and validation procedures for the temperature and concentration have been developed for the measurement of the release of trace elements from biomass in previous works at the TUM Chair of Energy Systems. The ETV unit employed at the Chair of Energy Systems uses a solid sampling method for the ICP-OES. To analyze solid biomass samples, small quantities of 1 to 5 mg are weighed into a graphite carrier, which is introduced into a resistively heated graphite-tube furnace and heated to temperatures up to 3000 °C in an inert atmosphere. During operation, the temperature is measured with an integrated pyrometer. The evolving gas phase is continuously transported out of the furnace by an Ar stream. Tetrafluoromethane (CF_4) is added to the carrier gas stream as it promotes halogenation, prevents the formation of carbides, and promotes nucleation to form aerosols, leading to higher signal intensities and more reproducible results. The carrier gas stream transporting the vaporized sample is mixed with an Ar bypass gas stream, leading to a temperature drop and the evaporated compounds become oversaturated and condense. Due to the gas flow conditions in this regime, a dry aerosol is formed. The aerosol is then led into the ICP-OES through a PTFE tube. The setup, adapted from the manufacturer, is shown inFigure 4 .

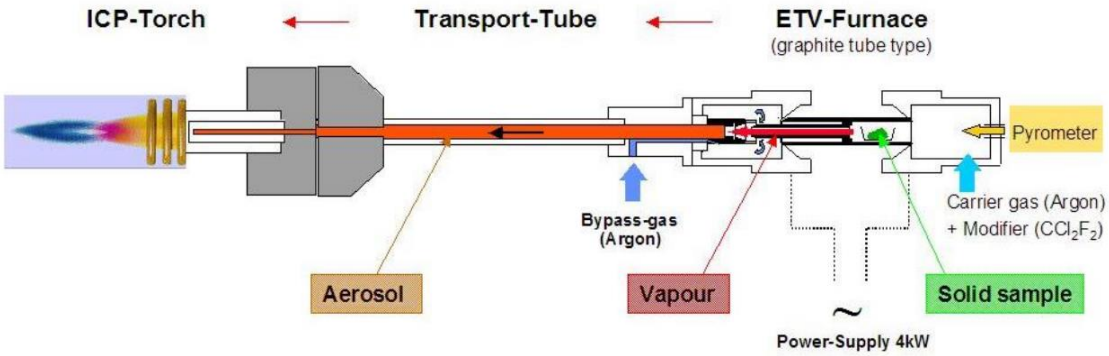

Figure 4: Schematic setup of the electrothermal vaporization unit (ETV) by Perzl, ETV 4000d Manual, Spectral Systems.

Short measurement times due to the simultaneous measurement of multiple elements at the same time, high versatility and productivity, and a large working range make ICP-OES an established and widespread technique for elemental analysis. ICP-OES is based on the excitement of atoms and ions in a plasma to emit electromagnetic radiation, which is specific for each element, and the detection of the emitted light with spectral resolution. A plasma is an ionized gas and characterized by independent movement of electrons and ions. In technical appliances, Ar is commonly used as plasma gas because its electron shell can easily be polarized. Energy is transferred into the plasma by the alternating electromagnetic field of an induction coil, causing the independent motion of Ar+ ions and electrons and leading to temperatures of up to 10000 K.

The plasma torch of an ICP, made of quartz glass, has an outer diameter of around 20 mm and consists of three gas streams. A schematic drawing of the plasma torch of an ICP is shown in Figure 5 a). The outer gas stream is referred to as plasma gas or cooling gas. To achieve the most efficient cooling, the plasma gas flows

tangentially through the outer tube. The auxiliary gas stream in the intermediate tube ensures that the tangential flow of the plasma gas is kept up until shortly before the plasma and that the plasma is not too close to the tip of the injector, preventing it from getting too hot. The inner gas stream carries the probe in the form of an aerosol into the plasma through the injector. The probe always must be brought into the form of an aerosol, which can be achieved in different ways. For the analysis of liquid samples, aerosols are created in a nebulizer, while a dry aerosol is directly formed inside the ETV (see above).

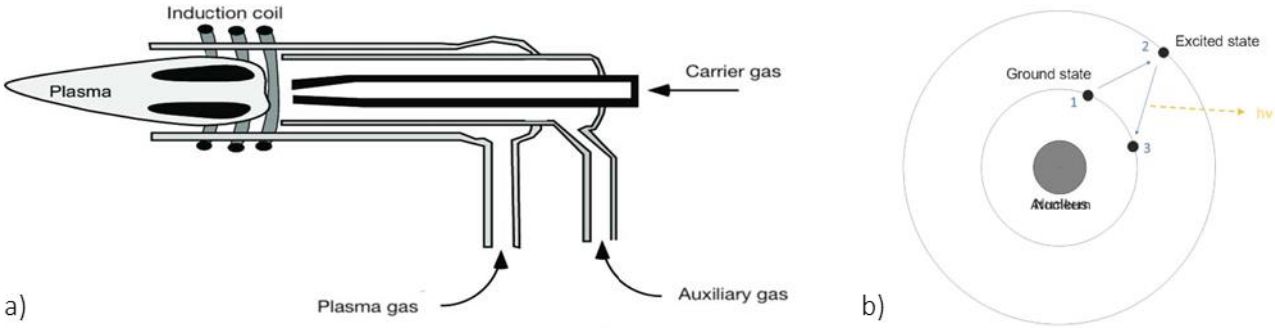

Figure 5: Schematics of: a) gas flows in an ICP plasma torch, and b) excitement of a valence electron in the plasma torch

Upon entry into the plasma, energy is transferred from the plasma to the sample in the following ways. First, the aerosol is dried, then the solids melt and evaporate. The gas molecules are now dissociated into atoms and, if the energy is sufficient, into ions. In typical ICP conditions, metals are dissociated into ions while nonmetals and metalloids are only partly ionized. Any surplus energy is used to excite valence electrons of an atom or ion, i.e. lift it into a higher orbital. After fractions of a second, the electrons fall back into a lower energy level, thereby emitting energy in the form of electromagnetic radiation. This process is shown schematically in Figure 5 b). The energy of the different states of electrons is specific for the element. The emitted energy in the form of light, which is equal to the energy difference of the excited state and lower state, is specific for each element and can be calculated with the Planck-Einstein relation. The emitted light is detected by the ICP-OES with spectral resolution. The wavelengths are used for the detection of an element, while the intensity of the wavelength is proportional to the concentration of the corresponding element.

2.3.2. Wire Mesh Reactor (WMR)

Experiments on the wire mesh reactor (WMR) were conducted at TUM-CES to analyze the reaction kinetics of gasification of feedstock under the EFG conditions, and the influence of released critical trace substances on subsequent gas purification. In addition, pretests to investigate the grinding behavior and handling (d_{max} < 250 µm and $d_{50} \approx 70$ µm), probe preparation, fuel feeding, and physical and chemical characteristics of treated and untreated fuels were conducted.

The WMR is used for the investigation of biomass devolatilization at high heating rates. In the GOLD project, additionally the residues of discrete measuring points at temperatures between 600 and 1200 °C are analyzed in the ICP-OES to measure the release of heavy metals. Figure 6 shows the WMR experimental setup and technical specification.

In the WMR, about 30 mg of a solid sample is given into a stainless-steel mesh, which is clamped between two electrodes. Two layers of the mesh are placed on top of each other, and the mesh is welded together on the sides, forming a bag which can contain the sample. The mesh is heated electrically, and the two wires of a thermocouple are welded on top of the mesh to measure its temperature. The temperature is adjusted by controlling the power supply. This setup is placed inside a metal box and the mesh is continuously swept by an inert N_2 stream to remove the volatiles from the sample preventing recondensation on the char. Biomass

samples are supplied o the mesh, dried together with the mesh at a temperature slightly above 100 °C, and weighed. A temperature of each measuring point is approached with a heating rate of 1000 °C and held for a certain residence time. After the experiment, the mesh and residue are dried again and weighed.

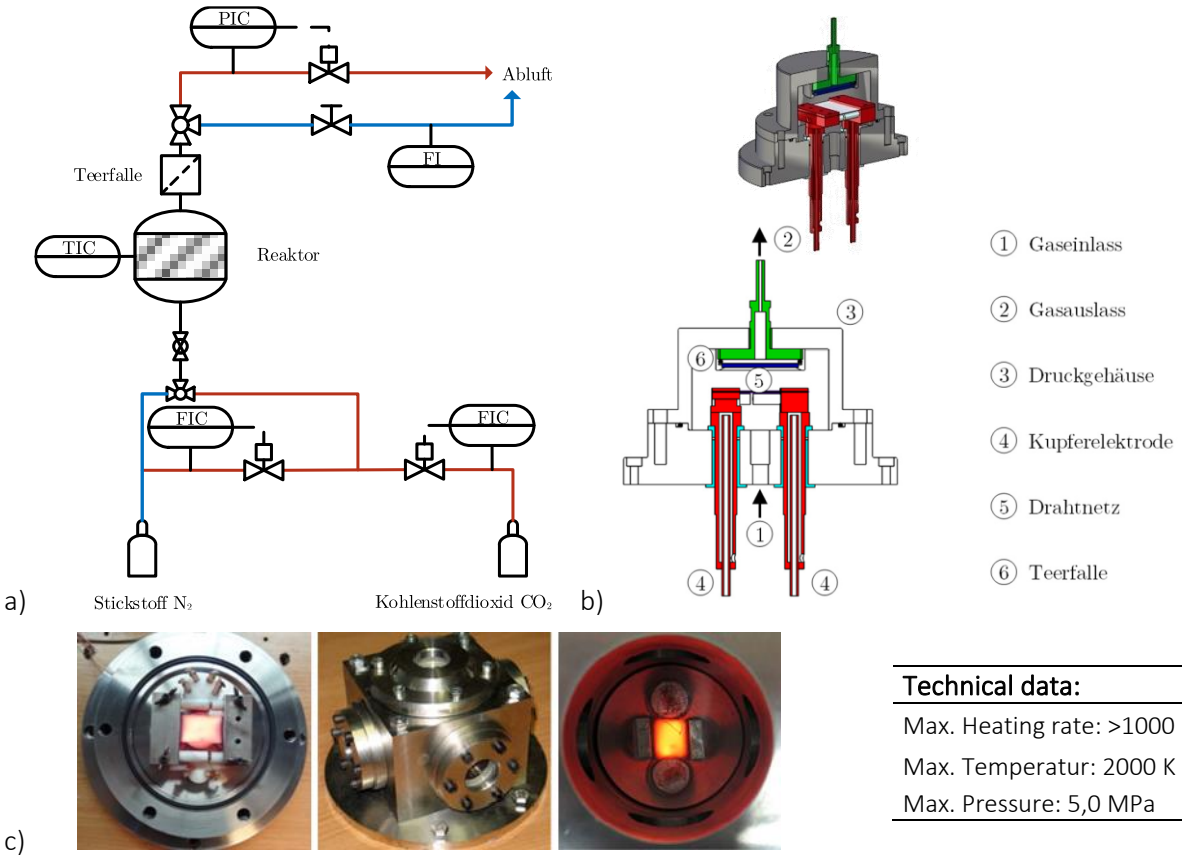

Figure 6: Wire mesh reactor (WMR) setup at the TUM Chair of Energy systems to analyze the reaction kinetics of biomass gasification: a) Process flow diagram [Geißler, 2020], b) Schematic structure [Steibel, 2018,], c) Images and technical data of the WMR.

WMR experiments are conducted at atmospheric pressure with torrefied and the two types of pyrolyzed sorghum. The design of experiment is shown inTable 4. After each measuring point, the sample and mesh are dried again and weighed. Each measuring point is repeated at least five times and the mean volatile yield is calculated while neglecting the two values with the highest deviation from the median. In the case of oxidative pyrolyzed sorghum, measuring points at 600 °C with a volatile yield that above 10% of the mean yield at 1000 °C are considered physically impossible and therefore neglected. All residues from the experiments at one measuring point are combined and the heavy-metal concentrations are measured using ICP-OES.

Table 4: Experimental plan for Sorghum WMR trials. T = torrefied (TNO), Po = oxidative- (RE-CORD), Pi = inert pyrolyzed (RE-CORD).

	Temperature in ˝C			
Residence time in s	**600**	**800**	**1000**	**1200**
1	T	T	T	
2	T	T	T	
5	T	T	T	
10	T, Po, Pi	T, Po, Pi	T, Po, Pi	T, Po, Pi

2.3.3. Baby High Temperature Entrained Flow Reactor (BabiTER)

EFG experiments at atmospheric pressure are conducted with the Baby High Temperature Entrained Flow Reactor (BabiTER) at the Chair of Energy Systems as shown in Figure 7 The reactor consists of a ceramic reaction tube made of Al_2O_3 with a length of 1.48 m and a diameter of 40 mm. The reaction tube is surrounded by three heating zones, each consisting of four heating elements. Different reaction gases are premixed in a gas collection tube and preheated in a 0.8 m long, and 25 mm thick horizontal ceramic tube surrounded by an electrical resistance heater. In GOLD WP2, N_2 and O_2 are used, and the amount of $O_2$is adjusted so that a prior specified equivalence ratio is achieved in the reaction tube.

Pulverized fuel is fed to the reaction tube from a dosing system at the top of the reactor, where a constant mass flow of the fuel is achieved by a combination of screw feeder and vibrational chute. The dosing system is enclosed in a container and nitrogen is fed into the container to prevent air from entering the reactor on this path and as carrier gas for the fuel. After leaving the reactor, the hot gas and particle mixture is cooled in a water quench with the constant removal of gas and quench water. Particle and gas samples can be taken out of the reaction zone with a sampling probe at an adjustable yet specified height inside the reactor tube, allowing for different residence times to be set.

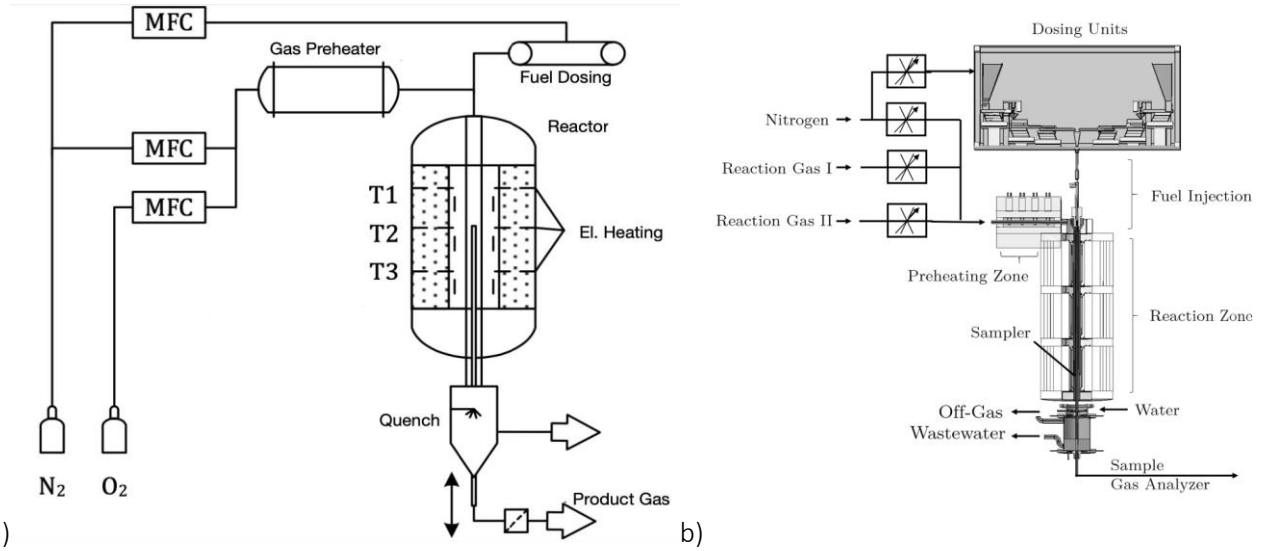

Figure 7: Simplified flowchart of the entrained-flow gasifier BabiTER: a) [Briesemeister et al., 2017], b) [Netter et al. 2021].

Like in the WMR experiments, the residues from discrete measuring points, which are collected during the experiment with the sampling probe, are analyzed in the ICP-OES to measure the release of heavy metals. For each biomass, gasification trials are conducted at four temperatures between 800 and 1100 °C in 100°C steps. The sampling probe is set to a height so that the particles are collected 1 m below the start of the reaction tube corresponding to gas residence times of 2.5 s and 1.37 6s real residence time for particles until removal. The conversion is calculated using the ash-tracing method. In addition, the BabiTER trials allow more detailed investigation of the biomass preparation, fuel feeding, handling (d_{max} < 250 µm and d_{50} ≈ 70 µm), and physical and chemical characteristics of treated and untreated fuels.

2.3.4. Gasification Kinetics

TUM-CES uses a Single First Order Reaction Model (SFOR) for the analysis of the volatile yield during gasification with only few parameters, based on the assumption of a first-order reaction. The SFOR assumes that the concentration of the volatiles c_v decreases in a linear correlation with increasing temperature. The reaction rate constant k of a first-order reaction is calculated using the Arrhenius equation. The pressure dependence of the volatile yield is neglected in this work. The combined influence of the temperature and residence time on the volatile yield $Y_V(t,T)$ is:

$$Y_V(t,T) = Y_{V,\mathrm{T_{set}}} + \left(Y_{V,\mathrm{T_{max}}} - Y_{V,\mathrm{T_{set}}}\right) \cdot \left(1 - e^{-\theta\cdot(T-T_{set})}\right) \cdot \left(1 - \exp\left(-k_0 \cdot \left(e^{-\frac{E_A}{RT}}\right) \cdot t\right)\right)$$

where T_{max} is the highest investigated temperature, T_{set} is a set temperature smaller than T_{max}, R is the universal gas constant, and T is the temperature. The thermodynamic parameter θ is fitted to experimental data by the method of the least square error and the kinetic parameters k_0 and the activation energy E_A are calculated.

2.3.5. General Experimental Limitations and Challenges

There are several challenges related to the experimental setup for EFG and the collection of data on heavy metal release. First, the uncertainty of the fuel analysis impacts all methods. The proximate and ultimate analysis and heating values are measured reproducibly, while little deviations are expected due to the inhomogeneity of biomasses. In the analysis of the heavy metals and metalloids in the ICP-OES, higher deviations are observed for some elements. According to a meta-analysis conducted in the GOLD project, the highest uncertainties of the heavy metals investigated in this work are detected for nickel (Ni) and titanium (Ti). The mean squared error of the concentration of Ni determined in different analyses, for example, is greater than 80%. In a few cases, high deviations are also observed for arsenic (As), cadmium (Cd), and copper (Cu). Chromium (Cr), iron (Fe), and lead (Pb) show reasonable deviations and the best results are obtained for manganese (Mn) and zinc (Zn).

The inhomogeneity of the biomass also affects the other methods, especially ETV and WMR due to little sample sizes (see Section 4.5). Further sources of errors include the measurement and control of the temperature in the ETV and WMR, and irregularities in the dosing system of the BabiTER, leading to a change in the reaction environment. Reliable and reproducible results are produced, while an uncertainty of the results, mainly due to inhomogeneities in the biomass and deviations in the measuring process, always must be considered. Especially the detection of elements with small concentrations, as seen for example for Cd and Ni, in the ICP-OES, for both liquid sampling in the laboratory analysis and the measurement with ETV-ICP-OES, is challenging due to the high background noise compared to the intensity of the measuring signal. Milling and homogenization of the biomass before measurements and analysis is always recommended.

3. Process Configurations, Syngas Cleaning & Conditions based on Process Modelling

3.1. Process Model Design

In addition to the removal of trace substances, especially heavy metals, the main gas composition after gasification is of decisive interest for the subsequent syngas fermentation. The interaction of these two main conversion processes also determines the performance of the overall process. The crucial link here is gas cleaning and purification. For a GOLD BtL route to become economically viable in the long term, the overall process must be considered as such. A process simulation offers the possibility to consider not only the interaction of the unit operations connected in series, but also various process-side optimization options that cannot be represented experimentally, such as industrial scale entrained flow gasification.

Thus, a process model was developed in Aspen Plus based on the process design developed as part of the GOLD project thermochemical Route 1. The base case model shown in Figure 8 uses drying, torrefaction and milling as pretreatment option, followed by oxygen-blown entrained flow gasification and a full water quench. Slag separation, and gas cleaning via water scrubber, cyclone and hot gas filter is included. Adsorptive gas cleaning is employed and H_2 and CO_2 are removed from the main syngas stream using PSA. The final synthesis to produce higher alcohols via syngas fermentation is modelled in a continuous stirred tank reactor (CSTR) using TUM-CBE derived gas fermentation kinetics.

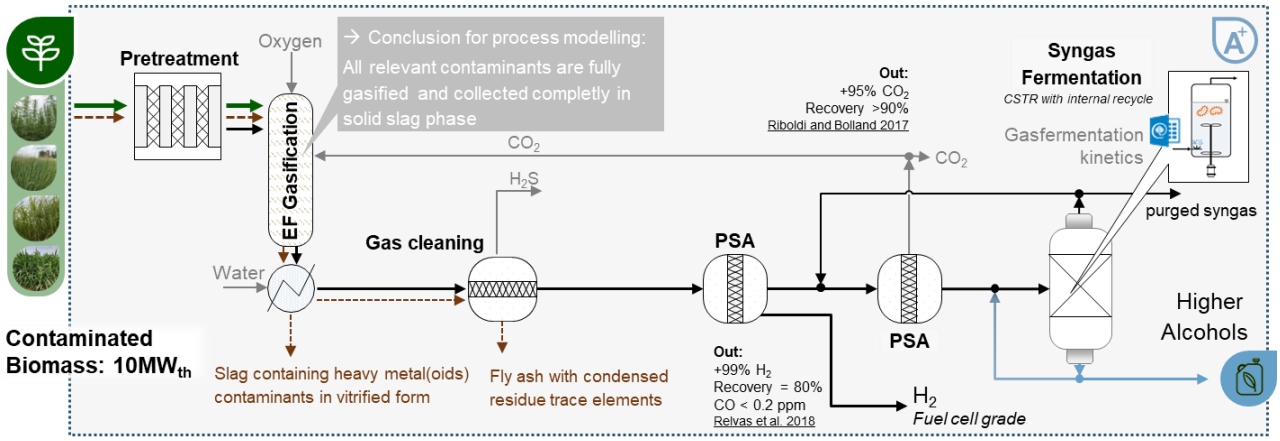

Figure 8: Simplified flowsheet of Aspen Plus base case reference model of GOLD Route 1 including torrefaction, entrained flow gasification and full water quench, adsorptive gas cleaning, H_2 and CO_2 separation via pressure-swing adsorption (PSA) and syngas fermentation in a continuous stirred tank reactor (CSTR) with gas and liquid recycle applying TUM-CBE-derived gas fermentation kinetics [Dossow et al., 2023].

Since the developed process model contains more than eight hierarchy units with multiple unit operations nested within, a detailed description of all process steps is not provided here. The process model is based on the biomass-to-syngas train including gas cleaning developed in [Dossow et al., 2021]. The oxygen-blown EFG (T_{EFG}=1400 °C) biomass input is specified as 10 MW_{th} representing a feasible scale for the process based on a preliminary analysis (see Section 3.1.3). Based on the findings from experimental gasification trials and thermodynamic modelling (see Section 4), it is assumed that all relevant contaminants are fully gasified in EFG and later completely collected during solid removal. Subsequent PSA steps are based on [Riboldi and Bolland 2017, Relvas et al., 2018]. The final syngas fermentation is modelled using kinetics based on TUM-CBE experimental data from [Doll 2018] applied to a CSTR with internal and external recycle design. For more details of the process technologies involved, see Section 2.1.

As the torrefaction, syngas cleaning and fermentation models are characterized by their specific design for the GOLD process, they are explained in more detail below. After the base case model is completed, optimization efforts were made to improve the overall process performance. This mainly includes overall energy yield, product yield, carbon efficiency and selectivity towards higher alcohols. The Aspen Plus GOLD route 1 model and its optimization was presented at EUBCE 2023 [Dossow et al. 2023].

3.1.1. Torrefaction Model and Validation

Key challenges affecting the feasibility of BtL projects include the low energy density and widely dispersed nature of biomass feedstock. To address these challenges, pretreatment is employed to enhance the energy density of the original biomass, reducing transport and storage costs. Typical pretreatment steps typically involve drying, torrefaction, and grinding of the biomass, with moisture content reduced during drying to 15% to optimize subsequent torrefaction and control parameters. Among various pretreatment methods for gasification, torrefaction demonstrates superior process efficiency and lower specific costs, including transportation to a central gasification facility. Torrefaction is a mild thermochemical pretreatment, to convert woody biomass into a high-energy-density, hydrophobic, compactable, and grindable product suitable for gasification. The process occurs isothermally in an inert environment at temperatures between 260°C and 300°C, resulting in devolatilization with an energy yield of up to 90% and a high volumetric energy density in the torrefied biomass. Beyond logistical benefits, torrefaction enhances the efficiency of biomass gasification.

The pretreatment design within the GOLD process model resembles an indirectly heated torrefaction process that uses waste heat from gasification. This has the advantage of reduced control complexity on the torrefaction level, while increasing overall process performance. Gaseous and solid torrefaction products are supplied to EFG maximizing carbon efficiency. Torrefaction is represented by a stoichiometric reactor (RStoic) simplified with regards to reaction kinetics, heat, and mass transfer limitations, and heat and pressure losses. In the reactor, biomass is converted into a densified solid product. It is assumed that no shrinkage or breakage occurs during torrefaction. Thus, the PSD of the torrefied biomass remains unchanged compared to that of the untreated biomass. The heat loss through the torrefaction reactor body is 0.5% of the HHV fed to torrefaction. The solid phase torrefied biomass is directed towards a grinder to be milled to below 300 µm.

During torrefaction, part of the dried biomass is devolatilized. The solid torrefied biomass leaves the reactor at a specified torrefaction temperature with a mass flow rate corresponding to the respective mass yield. The respective torrefaction temperature, as well as the moisture content after torrefaction, are specified. Torrefaction conditions at a temperature of 280°C and a moisture content after torrefaction of 1% are specified in accordance with GOLD TNO pretreatment trials.

In the simulation, the gaseous phase formed by the volatiles leaving the solid biomass consists of water (steam), carbon monoxide, carbon dioxide, methanol, acetic acid, formic and lactic acid. The related stoichiometric coefficients are calculated as the reciprocal of the molar mass to account for the molecular weight of 1.0g/mol of the nonconventional biomass. The fractional reaction extent of each reaction accounts for the respective yield. Since the extent of devolatilization increases with temperature and reaction time, the yield of the solid product decreases, whereas the yield of volatiles increases. Figure 9 shows the solid mass yield from torrefaction at various conditions on a dry and ash free basis. The model to determine the solid torrefaction mass yield depending on torrefaction temperature $\eta_M(T_{torr}$ *in °C)* is approximated by a second order polynomial best fit using the method of least squares for a 30min residence time to provide a conservative model according to:

$$\eta_{\mathrm{M}}(\mathrm{T_{torr}}) = \left(\frac{m_{torr,soild}}{m_{biom}}\right)_{daf} = -5.645 \cdot 10^{-5} \cdot T_{torr}^2 + 0.0239 \cdot T_{torr} - 1.5789$$

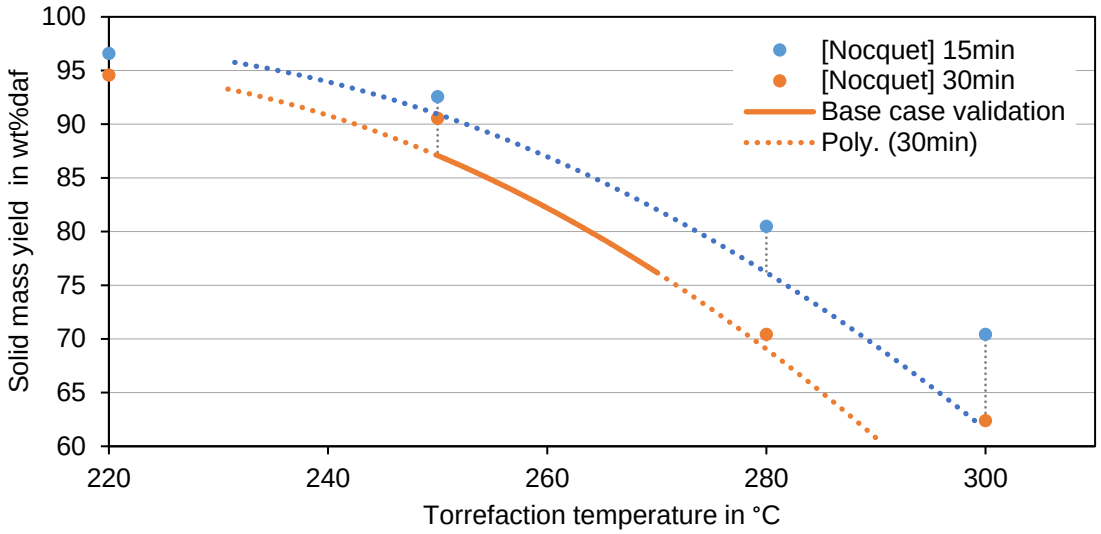

Figure 9: Yield of torrefied wood (widow and beech) as a function of temperature and residence time, from the kinetic model for torrefaction of willow at 15 min and 30 min residence time based on [Nocquet et al. 2014].

The composition of the gaseous products formed during torrefaction also varies with operating conditions. Figure 10 shows the dependency of volatile mass yield on temperature for the condensable gases water, formic acid, acetic acid, methanol and lactic acid and for the non-condensables CO_2 and CO. For the GOLD process model, the volatile yield is expressed as a function of temperature fitted to experimental data from [Prins et al. 2006, Nocquet et al. 2014]. The relationship between fractional conversion and temperature is expressed as a power function approximating the composition with reasonable accuracy.

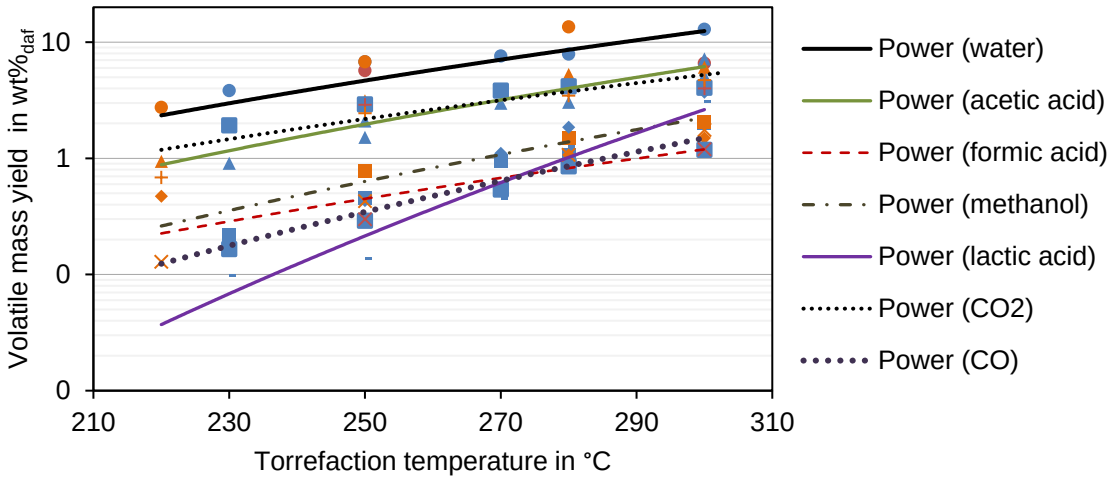

Figure 10: Volatiles yield from torrefaction of widow and beech as a function of temperature for different residence times, based on exp. data from [Prins et al. 2006, Nocquet et al. 2014].

The overall material balance is to be closed using an atom balance for the substances which are part of the ultimate analysis. The material balance can be closed if the moisture content before and after torrefaction is specified. Since the fixed-C content is not to be determined by the material balance, it is based on experimental data from TNO's samples after torrefaction is use. Similarly, HHV is taken from experimental results for Aspen to close the energy balance.

The experimental data from torrefaction at TNO is used to validate the model. TNO torrefaction pilot-scale trials of GOLD crops take place at 280 °C at a feeding rate of 2-3 kg/hr. Table 5 shows the comparison of experimental and modelling results for torrefaction using sorghum fuel analysis data from AUA/Lavrion site. The results indicate that, though the solid mass yield is not predicted at high accuracy, the main composition of the solid biomass in terms of C, H, N, S, O, Cl, is within an error margin of less than 12%. High deviations in ash content are due to the mass yield deviation while H is only present in small quantities resulting in high rel. errors for rather small absolute deviations. Based on this comparison, the developed torrefaction model is used in the Aspen Plus GOLD process model as described above.

Table 5: Comparison of experimental and modelling results for torrefaction of sorghum from AUA/Lavrion site including relative deviation on a dry basis in wt.%.

	TNO experimental	Aspen modelling	Rel. deviation
Solid mass yield	54.7%	68.6%	25%
Ash	17.10	10.96	-23%
C	53.03	53.41	1%
H	4.11	4.62	12%
N	1.57	1.43	-9%
S		0.24	
O	22.91	28.05	4%
Cl		1.29	

In this simulation, a Multiple Roll crusher type is selected using the U.S. Bureau of Mines breakage function at a mechanical efficiency of 90%. to model the milling of torrefied biomass to a maximum particle diameter of d < 300 µm, which is suitable for the subsequent EFG. Since the required grinding power is the main electrical power required in the pretreatment section, a generalized size reduction parameter of the feed material is selected. The Hardgrove grindability index (HGI) indicates the ease of grinding based on physical properties such as hardness, fracture, and tensile strength. It is commonly defined as a grindability parameter of brittle materials like coal. With torrefaction however transforming the fibrous biomass to a more brittle structure, the grindability indices are well suited to describe the grinding behavior of the torrefied biomass. Based on a linear fit to experimental data from [Manouchehrinejad et al., 2018] for torrefied biomass, the HGI value for simulation as a function of torrefaction temperature is given according to:

$$HGI = 0.1674 \cdot T_{torr} - 38.4$$

3.1.2. Syngas Cleaning and Purifaction

The configuration of the syngas cleaning step is subject to an iterative design process. Not only does the process depend on the syngas feed and its composition and pollution, but also on the syngas fermentation requirements downstream. Since an a priori estimation of the syngas composition is difficult and it is also unclear at this point in the project what purity must be achieved at all, the process design is based on experimental knowledge at the Chair of Energy Systems.

The TUM-CES commissioned a syngas cleaning test rig to be coupled with larger scale gasification equipment in 2023. The employed process technology can serve as a benchmark for future pilot scale experimental work. The plant includes a heated ceramic cartridge filter to remove particle impurities > 2 µm and a countercurrent packed water-based absorption column to separate water-soluble trace gas impurities and particles < 2 µm. The syngas is then cooled to 4.2 ± 0.6 °C using a glycol-cooled heat exchanger. After the moisture in the gas is

condensed, the final adsorptive purification step consists of four heated fixed-bed adsorption columns. [Rückel et al., 2022]

The selective adsorption train uses activated carbon at 45 °C to separate hydrocarbons, followed by an Al_2O_3 system to remove halogens at 160 °C. Adsorption column 3 uses ZnO for the removal of sulfur components at about 150 °C while a last catalytic activated carbon guard bed is operated at 45 °C. Additionally, a fifth reactor is operated at about 50 °C using a Pd-catalyst for the reduction of the O_2 in the syngas with the hydrogen to form water. The water is adsorbed into the silica gel beads to avoid condensation in the tube reactor or at the hydrophobic surface of the gas inlet sterile filter of the bioreactor. [Rückel et al., 2022]

An essential part of the project is the development of a gas purification system that meets the purity requirements for the synthesis gas for the subsequent gas fermentation. As described in Section 2.1.2, the targeted species to be removed from the syngas before fermentation are COS, H_2S, HCN, HCl, and all heavy metals. For this reason, a suitable gas purification structure is defined using HCl and NH_3 removal in a water scrubber, catalytic COS to H_2S conversion followed by removal H_2S via ZnO and HCN separation on activated coal. The enrichment of heavy metals and metalloids in bottom ash or slag, resulting in their immobilization and removal in non-leachable form (see Section 4), is considered in the slag removal and fly ash filter in the process model. Furthermore, a first PSA is used to separate H2 from the cleaned syngas. The process models a 4-step activated carbon for fuel cell grade H2 removal (+99% H_2, Recovery = 80%, CO < 0.2 ppm) based on [Relvas et al., 2018]. A second PSA removes CO_2 from the syngas. The 4-step PSA uses zeolite for high purity CO_2 (+95% CO_2, Recovery >90%) based on [Riboldi and Bolland 2017].

3.1.3. Syngas Fermentation

The syngas fermentation process design within the GOLD project's modelling framework uses syngas after gas cleaning and water as liquid phase representation. A CSTR model is employed in Aspen Plus to represent a continuously stirred tank bioreactor. This syngas fermentation section aims at a high conversion of the gasification-derived syngas into the desired product. However, the more negative Gibbs' free energy of the reactions with CO makes them thermodynamically preferable compared to CO_2 and H_2, resulting in a high preference to CO as the gaseous substrate for most acetogenic microorganisms [Rückel et al., 2022]. Thus, CO_2 and H_2 are only converted by acetogens when the concentration of dissolved CO decreases under a very low threshold and only CO converting reactions are considered in this work, as shown in Figure 11.

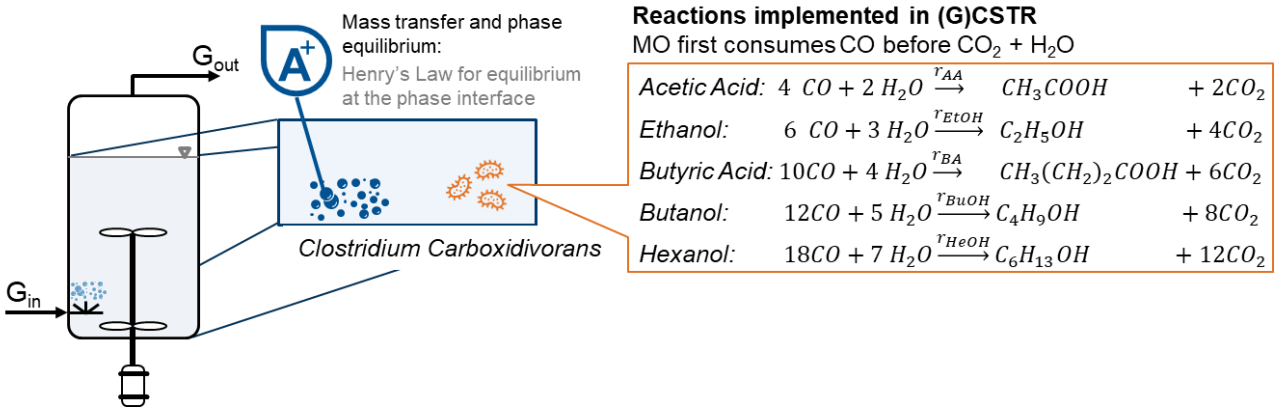

Figure 11:Model development and reaction equations inside a continuously gassed stirred tank reactor (CGSTR) [Dossow et al., 2023].

One of the main requirements of the thermodynamic CSTR model is the ability to represent the gas-liquid equilibrium of reactants and the products. Since the reaction takes place in the liquid phase, the thermodynamics method should predict the gas phase properties and consider both ideal and non-ideal behaviour of the liquid phase. NRTL-HOC property method meets this requirement and therefore is chosen for in this simulation model. This property method used the Hayden-O'Connell equation of state for the gas properties and the NRTL equation of state for the ideal and non-ideal liquid phase behaviour. NERL-HOC is also capable of predicting solvation of polar compounds and dimerization in the vapor phase. Additionally, *CO, CO_2, H_2* and *N_2* are added to Henry components list since they are non-condensable gases. [Dossow et al., 2023]

The production rate in the developed model is assumed to be a function two variables, the first of which is the CO concentration since CO is the limiting substrate in the reaction. The second variable is product concentration, which inhibits the reaction rate at higher product concentrations. The model fitting and calibration was done using experimental from [Doll 2018]. The dataset being limited to a continuously gassed stirred tank reactor (CGSTR) with CO input partial pressures varied between 0.2 and 1.0 bar at T = 37 °C; pH_0 = 6.0; P/V = 15.1 W/L; Gas flow = 5 L/h; V_R = 1.0 L). The following model assumptions were made to enable the fitting of the theoretical model to the experimental data [Dossow et al., 2023]:

- Product flow rate is equal to the average product concentration inside the CGSTR between day 4.5-6.
- No change in biomass concentration inside the GCSTR (biomass growth rate is equal to death rate).
- Feed stream of the reactor is assumed to contain *CO*, *CO_2* and *N_2* only.
- Ideal CGSTR with no temperature or concentration gradient.

The natural inhibition of the actual products must be considered in this CGST reactor, which is only continuously gassed, but no continuous liquid exchange is taking place. This means that the products are not discharged, they accumulate and then slow down the further production of the products. This would not be the case in a completely continuous STR, since the products are continuously discharged. Thus, like biomass growth, Monod kinetics with respect to CO for the individual reactions in the liquid phase, can serve as a baseline for reaction kinetic development. With r in mol/l/s, c_{CO} = concentration of CO at outlet, k as kinetic constants and K_s as the Monod constant, the substrate concentration where the rate is one-half the maximum, the following rate equation is derived:

$$r = -\frac{1}{v_i}\frac{dc_i}{dt} = \frac{r_i}{v_i} = k \cdot \frac{c_{CO}}{K_s + c_{CO}}$$

When inhibition is encountered, the inhibitor must be identified. Andrews kinetics was developed to take substrate inhibition into account (not to be confused with product inhibition). As mentioned above, we will not encounter substrate inhibition due to the low water solubility of CO. However, we could use the Andrews kinetic approach to account for product inhibition. Here, c_P accounts for the product concentration and is thus part of the kinetic equation, With K_L being the inhibition constant and w the sensitivity factor:

$$r = k \cdot \frac{c_{CO}}{K_s + c_{CO} + c_P \left(\frac{c_P}{K_I}\right)^w}$$

However, other formulations are possible besides the Andrews formulation when it comes to product inhibition. Levenspiel developed the following approach [Levenspiel 1980]:

$$r = k \cdot \left(1 - \frac{c_p}{c_P^*}\right)^n \cdot \frac{c_{CO}}{K_s + c_{CO}}$$

, where c_P^* is the limiting concentration of inhibitory product above which inhibition occurs and n is a constant. Han and Levenspiel also developed a more advanced following approach [Han and Levenspiel 1988]:

$$r = k \cdot \left(1 - \frac{c_p}{c_P^*}\right)^n \cdot \frac{c_{CO}}{K_s \left(1 - \frac{c_p}{c_P^*}\right)^m + c_{CO}}$$

Assuming n=1, this expression is developed into:

$$r = k \frac{\left(1 - \frac{c_p}{c_P^*}\right)^1 c_{CO}}{K_s + c_{CO}} = k \frac{1 - \frac{c_p}{c_P^*}}{1 + \frac{K_s}{c_{CO}}}$$

Based on these assumptions, the rate of product formation is described using:

$$r = k \cdot \frac{c_{CO}^1}{c_{CO} + \sum\left(K_{I,i} \cdot c_{P.i}^{w_i}\right)}$$

The following assumptions are made in the model:

- Acetic Acid only inhibits itself as it is also considered an intermediate in other products formation.
- Each products inhibits itself with $K_{I,i}$=1 and w_i=3
- Each product has a lower inhibition effect on other products than on itself. The inhibition constants of each product on other products is $K_{I,i}$=0.1 and w_i=4

The resulting kinetic rate expressions and kinetic constants are shown in Table 6.

Table 6: Reaction rate expression for all syngas fermentation products and fitted model constants used in the Aspen Plus CSTR LHHW reaction kinetic approach [Dossow et al., 2023].

Product	Reaction rate expression	Kinetic constants
Acetic Acid	$r_{AA} = k_{AA} \cdot \frac{c_{CO}}{c_{CO} + c_{P.AA}^3}$	$k_{AA} = 1.70 \cdot 10^{-7}$
Ethanol, Butyric Acid, Butanol, Hexanol	$r_j = k_j \cdot \frac{c_{CO}}{c_{CO} + c_{P.j}^3 + \sum(0.1 \cdot c_{P.i}^4)}$	$k_{Ethanol} = 1.00 \cdot 10^{-5}, k_{BA} = 3.60 \cdot 10^{-8}$, $k_{But} = 2.50 \cdot 10^{-7}, k_{Hex} = 7.00 \cdot 10^{-8}$,

As Aspen Plus CSTR models only allow a limited number of reaction kinetics types, a Langmuir-Hinshelwood-Hougen-Watson (LHHW) rate equation is selected here due to its wide flexibility. The LHHW kinetic expression consists of three terms, namely the kinetic factor, the driving force expression and the adsorption expression and it can be transformed into the following relation:

$$r = \frac{(kinetic\ factor)(driving\ force\ expression)}{(adsorption\ term)} = \left(kT^n e^{-\frac{E}{RT}}\right) \frac{(driving\ force\ expression)}{(adsorption\ term)}$$

$$r = k \frac{(driving\ force\ expression)}{(adsorption\ term)} = k \frac{k_1 \prod c_i^{\alpha_i} - k_2 \prod c_j^{\beta_j}}{\left[\sum_{i=1}^{M} K_i \left(\prod c_j^{\nu_j}\right)\right]^m}$$

Assuming the kinetic factor being constant over temperature. If $k_1 = 1,\ \alpha_i = 0,\ k_2 = \frac{1}{c_P^*},\ \beta_{j \neq P} = 0,\ \beta_P = 1, M = 2,\ K_1 = 1, \nu_j(i=1) = 0, K_2 = K_S, \nu_{j \neq CO}(i=2) = 0, \nu_{CO}(i=2) = -1, m = 1$, the expression can be simplified for each reaction according to Table 6.

The results of the simulation model fit to experimental data show relatively good agreement. The resulting sum of square roots SSR between the products flow rates in the model and the experimental data as well as the calculated R^2 values are calculated. Acetic acid shows a relatively low regression with R^2 value of 0.486, the other four products on the other hand show a good regression with R2 values ranging from 0.711 to 0.812. The reason for this can be the high variance and the limited number of the experimental data points for acetic acid, which are only four points. Nonetheless, the developed model is used in the following allowing a semi-mechanistic, CO, product, and volume sensitive modelling approach. [Dossow et al., 2023]

In the implemented CSTR model for the BtL process, the reactor volume plays a crucial role in determining the overall conversion and yield. Scaling up the reactor to a larger volume theoretically allows for achieving complete conversion of biomass. However, such scaling is often economically impractical. Increasing reactor size, while adhering to the principle of economy of scale, leads to escalated capital costs and higher operational expenses due to the stirring requirements inherent in CSTR operation. Furthermore, there exists a technological limitation on the maximum size achievable for stirred bioreactors, typically capped around 300 m³ [Meyer et al. 2016]. Simultaneously, the extent of conversion within the bioreactor and the design of downstream product separation processes significantly impacts both upstream gasification and gas cleaning operations. In an iterative approach, a rational gasification size was determined, corresponding to an appropriate number of bioreactors. Preliminary analysis indicates that a BtL model with a biomass input of 10 MW_{th} represents a feasible scale for the process. Reactor conditions inside the CSTR were controlled at p=const=1 bar, T=const=37 °C, pH=const=6, τ_l=8h , τ_g=1h. [Dossow et al., 2023]

Given that commercial companies implement a nutrient medium recirculation strategy in their plant designs, a similar approach is adopted in this study. Specifically, 70% of the cultivation medium is recirculated in practice. Therefore, a 70% recirculation of the liquid phase after fermentation is implemented in our setup. On the gas side, a portion of the unconverted syngas is reintroduced directly into the bioreactor. Given that the model does not account for the conversion of CO_2 and additional CO_2 is generated during fermentation, it is advantageous to remove this CO_2 before it enters the bioreactor. This not only reduces the volume requirements of the reactor but also enhances the partial pressure of CO. The resulting reactor configuration is shown in Figure 12. Through an iterative process optimization, a gaseous recycle rate of approximately 82% was determined using PSA to remove CO_2 prior to fermentation. Figure 12 also shows the CSTR fermentation model using an internal 70% gas recycle while another 15% are recycled to the rWGS instead. This design proved beneficial in terms of overall process efficiency when a rWGS unit is employed as described in more detail in Section 3.1.

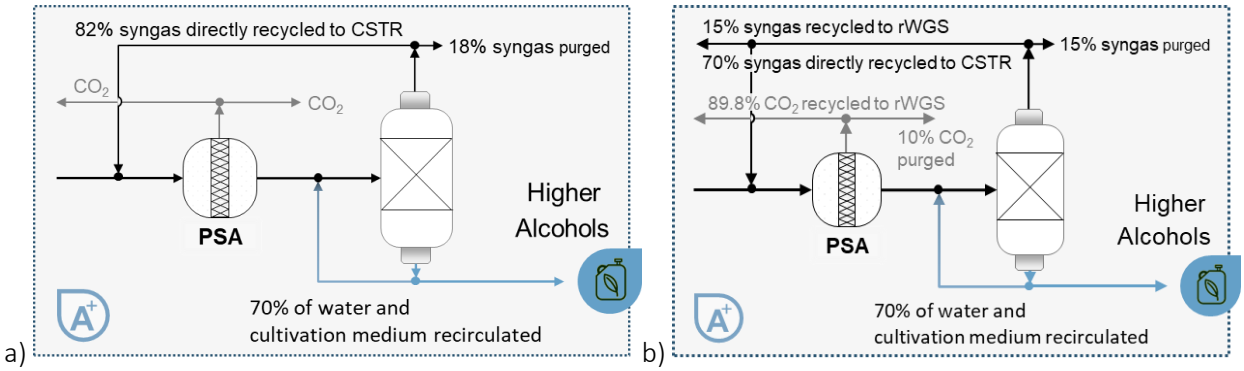

Figure 12: Syngas fermentation model using a continuously stirred tank reactor (CSTR) with internal recycle for a) "once through" and b) performance optimized overall process design [Dossow et al., 2023].

3.2. Process Model Results

The process model designed by TUM-CES within the GOLD project aims to evaluate the interaction of the major equipment, taking into account the experimental results, while optimizing overall process design. Using the general model framework and the detailed models described above and in [Dossow et al. 2021], a base case model was designed. The so-called "once-Through" model design is characterized by an internal syngas recycle for syngas fermentation (see also Section 3.1.3) separating H_2 and CO_2 from the syngas stream via PSA before synthesis as described in Section 3.2.1. Applying the learnings from experimental work and process development, the model is further optimized in terms of overall key performance indicators (KPI) such as product and energy yield, carbon efficiency and energy efficiency. The resulting design is shown in Figure 14 and discussed in Section 3.2.2.

3.2.1. "Once-Through" Model

As shown in Figure 8, in the base case of the "once-through" model, unconverted syngas is not fed back into the gasification reactor. However, a small part of the CO_2 separated in the PSA is used as carrier gas in EFG. The syngas fermentation bioreactor is sized to 4800 m^3 to ensure 95% CO conversion. With a maximum CSTR scale of 300 m^3, that results in a train of 16 gas fermenters. Since each reactor has a specific power requirement of 2 kWel/m^3 for stirring purposes, an overall installed stirrer power of about 10 MW_{el} is required.

Figure 13 shows the process model results in terms of KPIs. It can be shown that, despite the almost complete CO conversion in syngas fermentation, carbon efficiency is limited to 29%. This is mainly because CO_2 is not converted in the process. Furthermore, the stoichiometry for the sole autotrophic conversion of CO leads to the release of 1 mol CO_2 per 2 mol CO for acetate production and 1 mol CO_2 per 1.5 mol CO for ethanol production [Rückel et al., 2022]. Therefore, not all CO is converted into liquid valuable product while the CO_2 content increases.

The overall achieved product yield is 0.28 $t_{product}/t_{Biom,dry}$ (0.25 $t_{alc}/t_{Biom,dry}$ + 0.03 $t_{H2}/t_{Biom,dry}$), if H_2 is considered a by-product. In absolute numbers, a product yield of ethanol, acetic acid, butyric acid, butanol and hexanol of 523 kg/h and another 58 kg/h H_2 can be achieved, with a high selectivity towards ethanol. From an energetic point of view, that corresponds to an overall energy yield of 58.8%. If H_2 which in the employed model cannot be converted to biofuels in fermentation, wasn't part of the product mix, liquid energy yield would be reduced to 0.39 $MJ_{alc}/MJ_{Biom,dry}$ (0.19 $MJ_{H2}/MJ_{Biom,dry}$). In any case, 42% of the initial energy in the biomass is lost to the environment, mostly in the form of unconverted syngas and heat losses in gasification. If CSTR power requirements were included in the analysis, energy efficiency based on all products would be about 30% or 20% for only liquid products.

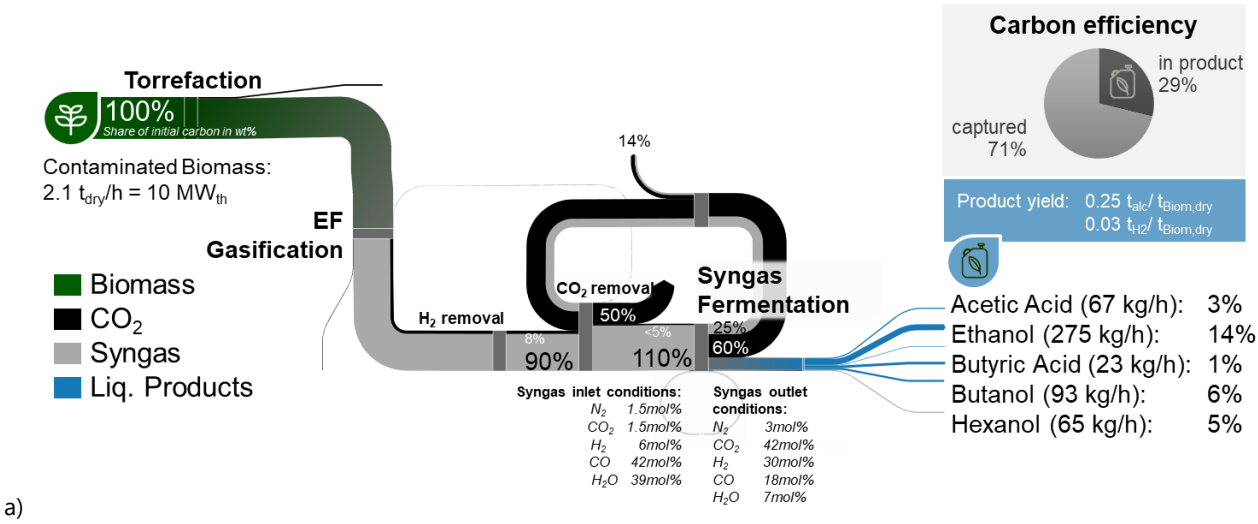

a)

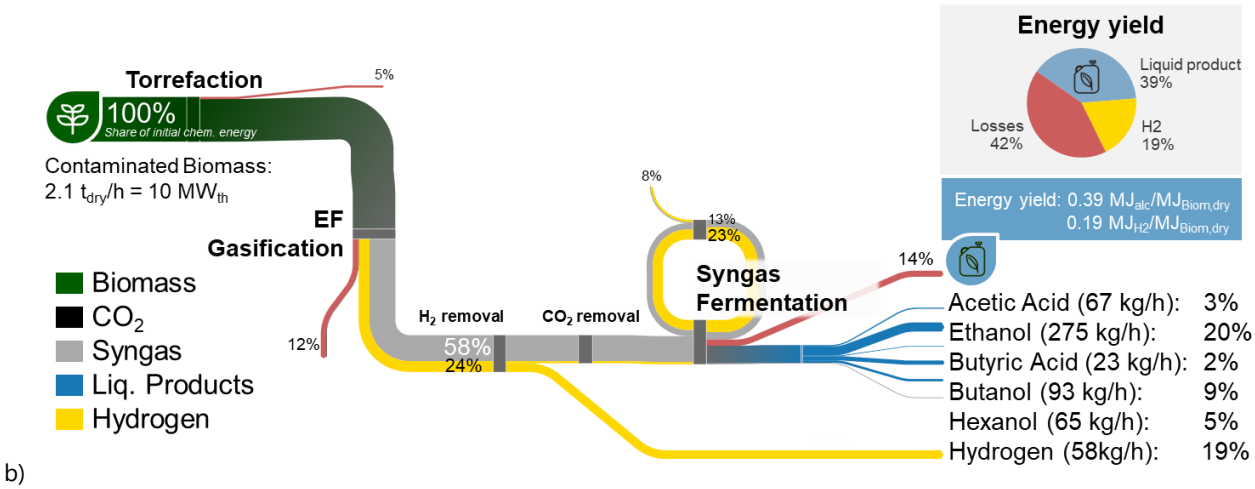

b)

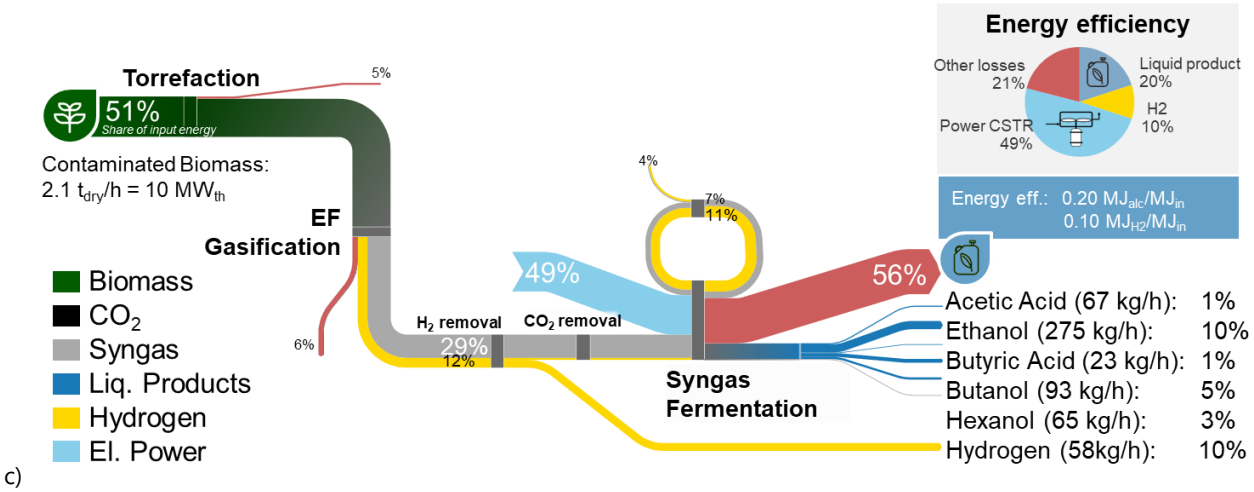

c)

Figure 13: "Once-Through" BtL model results in terms of a) carbon flow, efficiency and product yield, b) energy flow and yield and c) energy efficiency accounting for CSTR stirring power requirements [Dossow et al., 2023].

3.2.2. Performance Optimized Process Design

To increase product and energy yield, especially of the liquid product fraction, the process was optimized with respect to liquid fuel production capacity while maintaining biomass input at 10 MW_{th}. Optimizing the overall process flow and integration involves examining how different unit operations and process steps interact with each other. By reconfiguring the sequence of operations or integrating certain steps, the process can be streamlined, reducing energy and material losses, while improving overall efficiency. Similarly, mass integration focuses on optimizing the flow and utilization of materials within the process.

Figure 14 shows the resulting optimized and integrated process model design. while the general Biomass-to-Syngas train remains unchanged, 15% of the unconverted syngas recycled from the fermentation reactor (see Figure 12) is supplied to an earlier stage of the process. Here, after gas cleaning, a reverse WGS reactor is used to convert H_2 and CO_2, that otherwise would not be used in syngas fermentation, into CO that now can serve as a substrate for the bio-reaction. As the rWGS follows an equilibrium approach at 800 °C heated by exhaust heat from gasification, the remaining H_2 and CO_2 is removed from the syngas before fermentation. The bioreactor is kept at a constant 4800 m^3 reactor volume based on the "once-through" model.

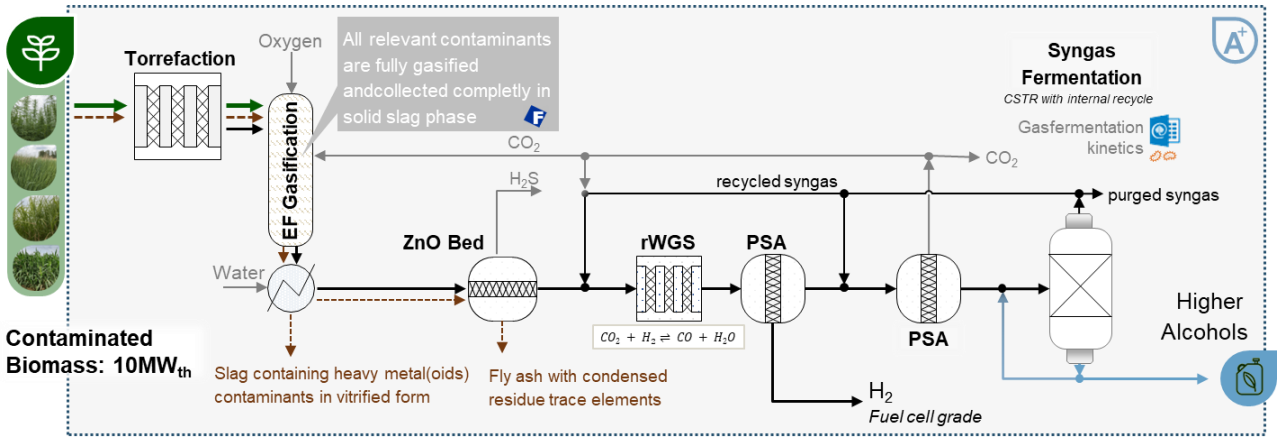

Figure 14: Simplified flowsheet of Aspen Plus optimized and integrated model of GOLD Route 1 including torrefaction, entrained flow gasification and full water quench, adsorptive gas cleaning using ZnO, reverse water-gas shit (rWGS), and H_2 and CO_2 separation via pressure-swing adsorption (PSA) and syngas fermentation in a continuous stirred tank reactor (CSTR) with internal and external recycle applying TUM-CBE derived gas fermentation kinetics [Dossow et al., 2023].

Figure 15 shows the process model results in terms of KPIs. Despite the slightly decreased overall CO conversion (now at 92% as opposed to 95% in "once-through" design), carbon efficiency is increased to 40%. The overall achieved product yield is 0.35 $t_{product}/t_{Biom,dry}$ with almost no H_2 present in the off-gases. In absolute numbers, a product yield of ethanol, acetic acid, butyric acid, butanol and hexanol of 728 kg/h is achieved. The high selectivity towards ethanol remains unchanged. Overall energy yield is slightly decreased from 58.8% to 55%. However, high-value biofuel energy yield is massively increased from 0.39 $MJ_{alc}/MJ_{Biom,dry}$ to 0.55 $MJ_{alc}/MJ_{Biom,dry}$. Still, 44% of the initial energy in the biomass is lost and energy efficiency is about 28% as CSTR power requirements are included in the analysis.

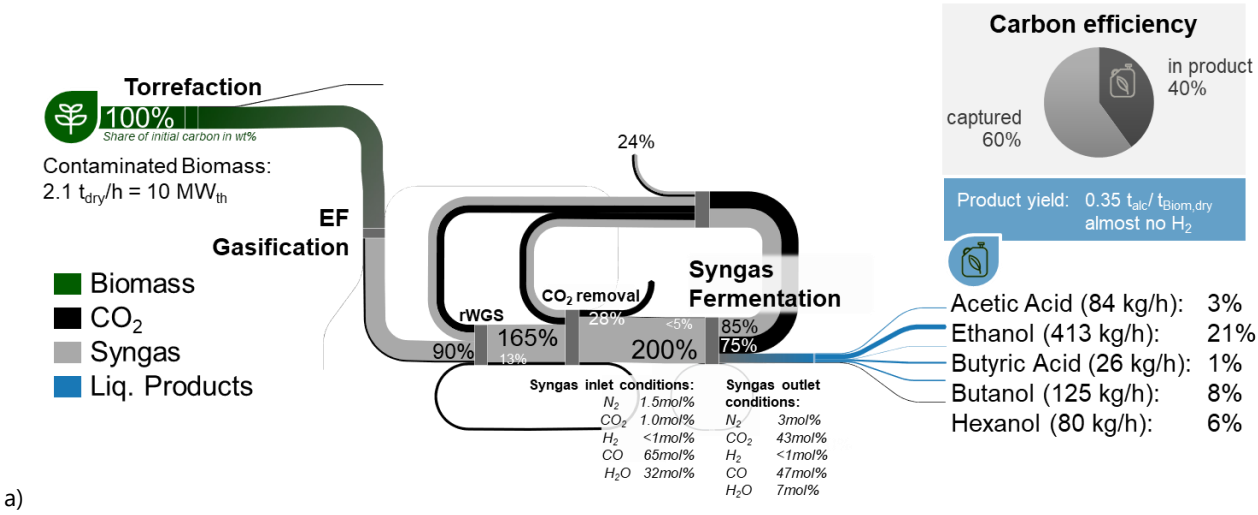

a)

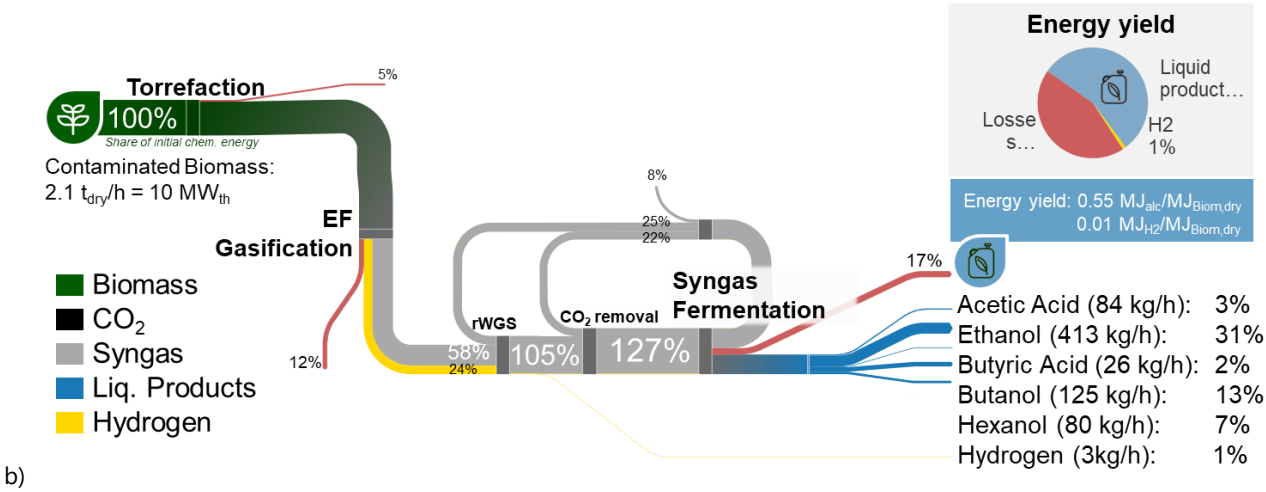

b)

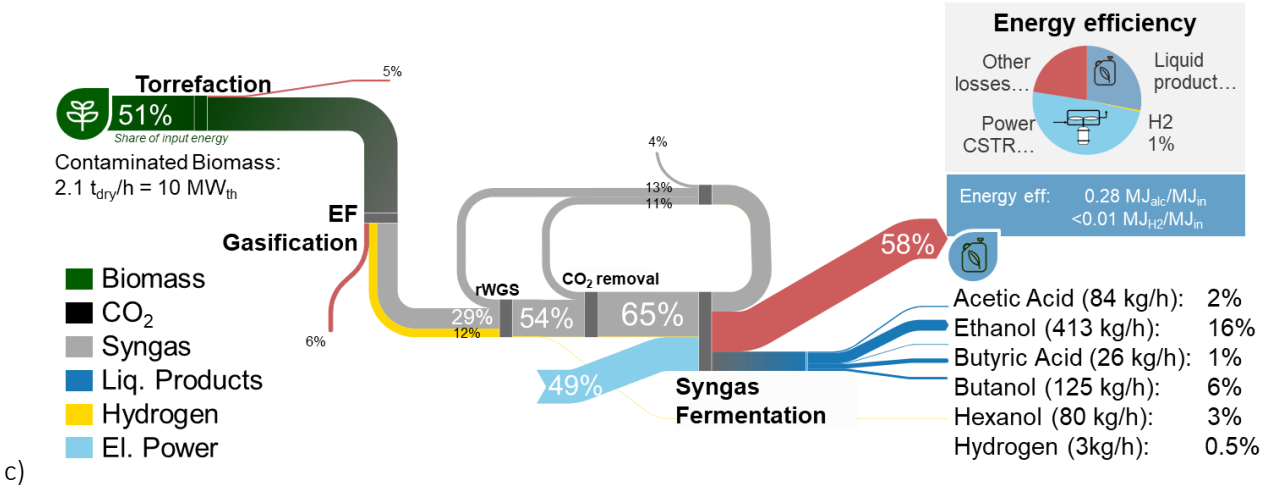

c)

Figure 15: Optimized and integrated BtL model results in terms of a) carbon flow, efficiency and product yield, b) energy flow and yield and c) energy efficiency accounting for CSTR stirring power requirements [Dossow et al., 2023].

Both process models show, that for industrial scale application, the power input by the stirrer to a stirred-tank bioreactor is typically the main operating expense. Thus, syngas fermentation on an industrial scale typically uses bubble column or gas-lift reactor due to the lower power input and more efficient syngas conversion high hydrostatic pressure of the water column allowing for higher solubilities of the syngas components at the bottom. Acetogen conversion of CO reduces the CO content in the rising gas bubbles over the height of the reactor, allowing a well-designed bubble column reactor to achieve high conversion of CO in the lower part of the reactor and subsequent conversion of CO_2 and H_2 in the upper part of the bubble column. [Rückel et al., 2022] Such an improved model, would not only require more data on CO_2 and H_2 as substrate in a continuous reactor setup, but also a BCR model that incorporates hydrostatic pressure for each height tray. One approach would be the use of Aspen Plus's RadFrac model allowing reactions to take place on every theoretical tray. Another way to further increase process performance is a cascade reactor network. This could be designed either as a cascade of bioreactors, each tailored for the respective gas feed composition, or as a cascade of bio- and chemical-catalytic reactors, that would make use of the H_2 and CO_2 rich off-gas of the reactor. However, such extensive modelling of the syngas fermentation process is out of scope for the GOLD project und subject to future work. Furthermore, the GOLD process based on the developed process model, could be investigated from a techno-economic and lifecycle perspective. As this is part of the WP3 work in GOLD, relevant process data is supplied to the respective partners.

3.3. Expected Syngas Conditions from GOLD Biomass

Syngas composition in terms of main substances CO, H_2, and CO_2, is a crucial aspect of syngas fermentation. As a majority of the N_2 and O_2 in real-life syngas from gasification is not produced during EFG but comes from the dosing amounts, purging processes, and safety valves [Rückel et al., 2022], a directly coupled industrial BtL process would not face problems related to N_2 or O_2 content in the used syngas.

As autotrophic CO conversion generates CO_2, an ideal biomass-derived syngas would require as little CO_2 as possible. High CO_2 concentrations in syngas from EFG mainly result from low product gas temperature at the end of the reactor (thermal losses and non-ideal quench geometry), unconverted biomass and generally poor rector design. An industrial EFG reactor would be almost CO_2 free. To achieve high conversion of CO_2 and H_2, the H_2/CO_2 ratio before fermentation must approach 2 for acetate and 3 for ethanol production. Thus, the ideal stoichiometric H_2/CO ratio in the syngas for total conversion of both components in a bubble column or gas-lift bioreactor would be 2 for ethanol production, and 1 for acetate production. [Rückel et al., 2022]

To estimate industrial-scale syngas compositions in terms of main components and close the mass balance for C, H, N, S from biomass-to-syngas, the biomass-to-syngas model as developed in [Dossow et al., 2021] is used. The model uses the minimization of Gibbs free energy to calculate gas phase chemical and phase equilibrium at given temperature and pressure. The feed stream to the gasifier model is based on the fuel analysis of the already pretreated biomass samples (torrefaction and torwash from TNO, inert and oxidative pyrolysis from RE-CORD). The EFG is scaled to 10 MW_{th} to represent a feasible scale (based on preliminary analysis in Section 3.1.3), and O_2 requirements are calculated to reach T_{EFG}=1400 °C. Table 7 shows the resulting syngas composition after gasification and quench, after gas cleaning, and just before entering the syngas fermentation bioreactor. All feedstocks are gasified at an equivalence ratio around 0.26-0.28. For pyrolzed sorghum, a steam addition of 0.17 $kg_{steam}/kg_{biomass}$ is necessary to ensure total conversion under EFG conditions. The resulting syngas is free of CO_2 and O_2 and shows a H_2/CO ratio of about 0.5 for torrefied and torwashed sorghum, and about 0.25 for pyrolyzed sorghum.

Table 7: Fuel analysis results for 2023 sorghum samples collected from the AUA field in Lavrion (MB2 samples) and pretreated via torrefaction, torwash (both TNO), inert or oxidative pyrolysis (both RE-CORD) and resulting syngas composition after gasification according to the Aspen Plus Model.

Proximate analysis		**Raw Sorghum (AUA)**			**Torrefied Sorghum (TNO)**			**Torwashed Sorghum (TNO)**			**Pyrolyzed Sorghum (inert) (RE-CORD)**			**Pyrolyzed Sorghum (oxidative) (RE-CORD)**		
		ar	dry	daf	ar	dry	daf	ar	dry	daf	ar	dry	daf	ar	dry	daf
H_2O	wt%	7.46	-	-	3.56	-	-	4.11	-	-	3.17	-	-	2.89	0.00	0.00
Volatiles	wt%	68.07	73.56	79.81	44.53	48.12	52.21	57.41	62.04	67.31	8.03	8.67	9.41	8.09	8.74	9.48
Ash	wt%	7.25	7.83	-	15.82	17.10	-	3.79	4.10	-	24.39	26.36	-	24.69	26.68	0.00
Fixed-C	wt%	17.16	18.54	20.12	32.19	34.79	37.74	31.30	33.82	36.70	60.12	64.97	70.49	59.76	64.58	70.07
Ultimate analysis																
C	wt%	38.86	41.99	45.56	49.07	53.03	57.54	52.34	56.56	61.36	60.14	64.99	70.51	59.56	64.36	69.83
H	wt%	5.35	5.78	6.27	3.81	4.11	4.46	4.54	4.91	5.33	0.68	0.74	0.80	0.79	0.85	0.92
N	wt%	0.95	1.02	1.11	1.45	1.57	1.70	1.09	1.17	1.27	1.35	1.45	1.58	1.41	1.53	1.66
S	wt%	0.16	0.17	0.18				0.08	0.09	0.10				0.00		0.00
O	wt%	39.13	42.28	45.88	22.39	24.19	26.25	30.37	32.81	35.60	5.98	6.46	7.01	6.09	6.58	7.14
Cl	wt%	0.86	0.92	1.00				0.33	0.35	0.38				0.00		0.00
HHV[a]	kJ/kg	15635	16896	18333	20660	22326	24224	21381	23105	25069	23136	25002	27127	23147	25014	27141

Syngas composition after gasification

			Gasification conditions			**Gasification conditions**			**Gasification conditions[c]**			**Gasification conditions**		
	ER	mol/mol	0.26			0.26			0.28			0.28		
	ROC	mol/mol	0.40			0.43			0.32			0.32		
			Raw	**Clean**	**Inlet**	**Raw**	**Clean**	**Inlet**	**Raw**	**Clean**	**Inlet**	**Raw**	**Clean**	**Inlet**
	CO_2	mol%	0.01	0.01	0.01	0.03	0.03	0.01	0.00	0.00	0.01	0.00	0.00	0.01
	H_2	mol%	0.15	0.15	0.20	0.16	0.16	0.21	0.08	0.08	0.10	0.09	0.09	0.10
	CO	mol%	0.31	0.31	0.44	0.29	0.29	0.42	0.35	0.35	0.46	0.35	0.35	0.46
	H_2O	mol%	0.52	0.52	0.32	0.52	0.52	0.34	0.55	0.55	0.31	0.55	0.55	0.31
	O_2	mol%	0.00	0.00	0.00	0.00	0.00	0.00	0.00	0.00	0.00	0.00	0.00	0.00
	N_2	mol%	0.00	0.00	0.02	0.00	0.00	0.02	0.00	0.00	0.02	0.00	0.00	0.02

[a] HHV analysis according to DIN51900-1
[b] Syngas composition: Raw: raw syngas after gasification + quench, Clean: after gas cleaning, Inlet: after mixing with recycle stream just before entering the syngas fermentation
[c] for pyrolzed sorghum, a steam addition of 0.17 $kg_{steam}/kg_{biomass}$ is necessary to ensure total conversion during gasification

4. Heavy Metal Contamination Content in Syngas, Slag and Ash of Gasification

As described in Section 2.1.2 of this report, it is expected that heavy metals and metalloids sublimate or react forming gaseous compounds in EFG eventually being enriched in:

- the bottom ash/slag in the gasification chamber, or
- the fly ash together with fine ash particles in the flue gas, or
- the flue gas and need to be removed in the gas cleaning system.

When heavy metals and metalloids are enriched in the bottom ash or slag, they are immobilized in a non-leachable vitrified form, which facilitates their management and disposal. The vitrification process essentially locks the contaminants into the solid matrix, reducing the risk of leaching into the environment. As a result, disposal of bottom ash or slag enriched with heavy metals and metalloids in non-leachable form is typically easier and safer compared to other forms of contamination. Proper handling and disposal methods remain important to ensure containment and prevent dispersion into the environment, but the inherent stability of the vitrified matrix minimizes the risk of environmental impact. Therefore, the enrichment of heavy metals and metalloids in bottom ash or slag is indeed a desired outcome in gasification processes aimed at managing these contaminants effectively. Regardless of the enrichment location, residues from downstream processes such as bottom ash, slag, fly ash, or captured contaminants need appropriate management, including storage, treatment, and disposal, to prevent environmental contamination.

The key elements of heavy metal release under gasification conditions are summarized in Section 2.1.2. To better understand that behavior, the phase transition from solid to gaseous is modeled within the GOLD project. To validate the model and show the actual fate of contaminations during gasification, experimental trials are conducted using the gasification test rigs ETV, WMR and BabiTER at TUM-CES.

4.1. Thermodynamic Phase Transition Model Predictions

Thermodynamic modelling in FactSage with the model described in Section 2.2 is carried out to model the temperature dependent phase transition behavior of heavy metals and metalloids during EFG and the water quench. Both, oxidative and inert gasification conditions are investigated. The input for the respective modelling consists of the fuel data and the operating conditions, the gasification temperature, i.e. equivalence ratio, is varied between 400 °C and 2400 °C. The validation and modelling results for EFG under oxygen-blown conditions are presented in the following.

4.1.1. Model Validation

The used databases in this work are FactPS, a database containing vast amounts of pure substance data. Additionally, solution databases containing data on solution phases can be combined with the component database. In this case, one of the used databases needs to be prioritized as they may contain different data for some species. Four different solution databases, GTOx, FToxid, FTsalt, and FTmisc, and many of their solution phases are investigated. Further, the gas phase is treated as real or ideal. The suitability of any combination of databases and settings was validated by reproducing the data created by [Jiang etal., 2016]. Jiang etal. (2016) modeled the phase transition temperature under atmospheric steam gasification conditions using the software MTDATA (NPL, United Kingdom). The considered heavy metals and metalloids are Al, As, Cd, Co, Cr, Cu, Fe, Mn, Mg, Ni, Pb, and Zn. The input parameters regarding temperature, pressure, elemental composition of the biomass, and gasifying agent are taken from [Jiang etal., 2016].

No variation proves to be superior to the others and every combination of databases and parameters shows relatively good agreement with the reference for some of the considered elements and relatively large deviations for others. According to the documentation by GTT-Technologies, GTOx is, among other things, especially suited for the modelling of slag formation, fouling, and condensation during biomass gasification. Therefore, a combination of FactPS and GTOx, an oxide database consisting of data for slag, liquid metal, and liquid sulfite as well as many solid solution and stoichiometric phases, is recommended for the modeling of slag formation, fouling, and condensation during biomass gasification by GTT-Technologies.

4.1.2. Release of Heavy Metals Modelling Results

The results for the simulation of the phase transition of the heavy metals and metalloids from the solid phase to the gas phase during EFG indicate that the release behavior of the heavy metals is similar in all investigated biomasses. Further, it shows that cadmium (Cd), lead (Pb), and zinc (Zn), are the volatile elements and are entirely volatilized at a temperature of 1800 °C, which is a typical temperature in the hot zone during EFG. Cd is volatilized at temperatures between 500 °C and 600 °C, while the volatilization of Pb occurs over a wider temperature range between 500 °C and 900 °C. Most of the Zn is volatilized between 800 °C and 100 °C. Then, the volatilization of Zn is delayed between roughly 1000 °C and 1500 °C due to the formation of a slag phase in this temperature range. Cu, which is only contained in raw sorghum, is volatilized between 900 °C and 1200 °C. during gasification

The other elements, namely nickel (Ni), iron (Fe), manganese (Mn), chromium (Cr), titanium (Ti), and vanadium (V), which is only contained in the raw sorghum, are non-volatile. Their volatilization doesn't considerably start at temperatures below 2000 °C and less than 10% of these elements is in the gas phase at the gasification temperature of 1800 °C. Mn is an exception to this, as it shows partial volatilization at lower temperatures in case of the two types of pyrolyzed sorghum, and Cr is also starting to volatilize at 1700 °C in the case of torwashed sorghum. Ti is the least volatile element and not substantially released in the investigated temperature range.

In the next step, the phase transition of the heavy metals and metalloids contained in the gas phase after the reaction zone to the solid phase during the water quench is simulated using the Scheil-Gulliver cooling approach. The results indicate that all mass fractions are given in relation to their total mass entering the water quench in the gas phase at 1800 °C. All semi-and non-volatile elements start to recondense immediately after leaving the hot zone. Only small amounts of Ni and Ti are in the gas phase entering the water quench and, in most cases, they immediately solidify.

The solidification of the other elements takes place over a wider temperature range, but all non-volatile elements, except for Mn and Fe, are entirely solidified at a temperature of 1000 °C. However, the formation of metal complexes and slag phases delays the solidification in many cases, leading to plateaus in the plot. This effect is especially pronounced for Mn and Fe, which is why a fraction of those two elements remains in the gas phase even at temperatures below 1000 °C in many cases. The volatile elements, on the other hand, start to solidify at temperatures below 90 °C. Zn starts to solidify first and is entirely solidified in the temperature range between 900 ° and 500 °C, apart from inertly pyrolyzed sorghum, where the solidification is delayed due to the formation of complexes. Cd is rapidly solidified between 600 °C and 400 °C. Pb solidifies between 800 °C and 400 °C, while the solidification is delayed in the case of the two types of pyrolyzed sorghum.

4.2. ETV-ICP Results

In the GOLD project, a method for the measurement of the release of the heavy metals cadmium (Cd), chromium (Cr), nickel (Ni), lead (Pb), and zinc (Zn) with the ETV-ICP system described in Section 2.3.1 is developed. The first step is the calibration of the temperature and concentration, followed by the validation.

4.2.1. ETV Temperature and Concentration Calibration and Validation

The temperature calibration is conducted by heating the ETV to 1000 °C and 2000 °C, respectively, and the temperature is measured with the internal and the external pyrometer. From the determined deviation, the settings of the internal pyrometer are adjusted via linear regression until the deviation of the pyrometers is less than 1%. The temperature validation is done before and after all measurements according to the procedure developed by [Mörtenkötter et al., 2024]. A sulfur single element standard is used for the validation in the lower temperature range and pure silver in the form of a wire is used for the upper temperature range. The concentration calibration is done with liquid ICP standard solutions according to the procedure described by [Mörtenkötter et al., 2024]. Single element standards are mixed to create a liquid multi-element standard. The composition of the multi-element standard must be in the same order of magnitude as the investigated biomass and is presented in Table 8.

Table 8: Composition of the multi-element standard for the calibration of the concentration. The investigated wavelength is also shown for the heavy metals, for argon as monitor, and for silver and sulfur for the temperature validation.

Element	Concentration in mg/L	Wavelength in nm
Ag		243.779
Al	300	
Ar		430
As	10	
Cd	10	214.438
Cr	10	357.869
Ni	10	231.604
P	300	
Pb	10	220.353
S		182.034
Zn	10	206.2

4.2.2. Release of Heavy Metals in ETV

As described in Section 2.3.1, the temperature-resolved release of the heavy metals Cd, Cr, Ni, Pb, and Zn from the biomasses is measured in this work by ETV coupled with ICP-OES. For this purpose, the total heavy metal concentrations in the biomass samples are determined and the mass fraction in the gas phase over the temperature is measured in the ETV-ICP-OES system. The elements Cd, Pb, and Zn are the volatile heavy metals in the ETV. Most of the Cd is released almost immediately at a temperature of 500 °C in the torrefied, torwashed, and raw sorghum. The volatilization of Cd in the case of the two types of pyrolyzed sorghum starts later at around 600 °C and takes on over a wider temperature range. Pb is entirely released quickly between 600 °C and 800 °C. The release of Zn also starts at a temperature of around 600 °C, but Zn is released over a wider temperature range compared to Pb. The release is especially slowed down between 1000 °C and 1500 °C, while most of the Zn has already been released from the biomasses at those temperatures. Cr and Ni show less volatile behavior in the ETV. Most of the Cr is released between 1500 °C and 1700 °C and most of the Ni between 1550 °C and 1750 °C. After that, their release is slower, and they are only entirely released at the final ETV temperature of 2400 °C.

4.3. WMR Results

As described in Section 2.3.2, the wire mesh reactor (WMR) is used in the GOLD project to conduct experiments with torrefied, inert pyrolyzed, and oxidative pyrolyzed sorghum from the AUA Lavrion field test site. Gasification kinetics are analyzed with the Single First Order Reaction Model (SFOR, see Section 2.3.4and the char residues are analyzed to measure the release of heavy metals during devolatilization.

4.3.1. SFOR Gasification Kinetics in WMR

The temperature dependence of the volatile yield of GOLD crops under EFG conditions is investigated for temperatures between 600 °C and 1200 °C in steps of 200 °C at atmospheric pressure, a heating rate of 1000 °K/s, and residence times between 1 and 10 s. The parameters of the SFOR are derived with the thermodynamic parameter θ being fitted to experimental data by the method of the least square error and the kinetic parameters k_0 and the activation energy E_A calculated (see Section 2.3.4). The results for the fitting of gasification parameters are shown in Table 9.

Table 9: Parameters of the Single First Order Reaction Model (SFOR) fit to data from WMR experiments of GOLD Sorghum from AUA.

Pretreatment method	θ	k_0 in s^{-1}	EA in kJ/mol
Torrefied (TNO)	0.0125	779.99	48.012
Pyrolyzed inert (RE-CORD)	0.005		
Pyrolyzed oxidative (RE-CORD)	0.0143		

The curves of the SFOR, which are plotted in Figure 16 a) are calculated at 600 °C. The volatile yields at 1200 °C are neglected for the SFOR, as they are likely influenced by secondary pyrolysis reactions occurring at higher temperatures, which can't be predicted with a first-order reaction model. Therefore, 1000 °C is T_{max}. Further, the SFOR curve of oxidative pyrolyzed sorghum is assumed to have the same zero point as the curve of inert pyrolyzed sorghum to receive a physically reasonable curve. For torrefied sorghum, the volatile yield increases from 44.3% at 60 °C to 58.4% at 800 °C and then remains on the same level for 1000 °C. At 1200 °C, the volatile yield is increased again to 67.8%. For inert pyrolyzed sorghum, the volatile yield is increased slowly between 600 ° and 1000 °C from 5.4% to 15.3%. The volatile yield at 1200 ° is 46.4% and therefore substantially higher than at 1000 °. For oxidative pyrolyzed sorghum, the volatile yield is constantly between 6% and 9% temperatures between 600 ° and 1000 °, while the volatile yield at 1200 ° is again substantially higher at 41.7%.

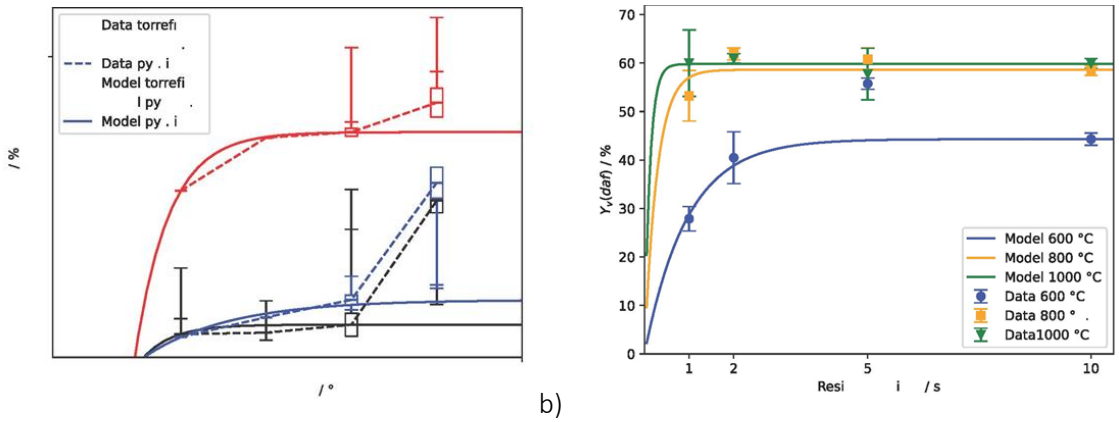

a) b)

Figure 16: Fitted SFOR model dependency of the volatile yield on a) temperature for torrefied (TNO) and pyrolyzed sorghum (RE-CORD), b) residence time during devolatilization for torrefied sorghum (TNO) from AUA in WMR.

Results suggest that, for the pyrolyzed sorghum, almost all volatiles have been driven out of the solid biomass structure during pretreatment already, while the volatile content in the torrefied sorghum is still high. Therefore, significant devolatilization is only observed for torrefied sorghum and the release of gases for the pyrolyzed sorghum is mainly due to the high heating rate. This is also why the volatile yield of the pyrolyzed sorghum shows only weak temperature dependence. The devolatilization of torrefied sorghum is finally completed at 800 °C. Yet, a big increase in volatile yield is observed from 1000 °C to 1200 °C for all biomasses. This is likely due to secondary pyrolysis reactions occurring at higher temperatures. The results for the kinetic parameters k_0 and E_A are used to derive the dependency of the volatile yield on the residence time. Fitting the volatile yield over the residence time for torrefied sorghum for residence times between 1s and 10s in the base case at temperatures of 600 °C, 800 °C, and 1000 °C,at atmospheric pressure, and a heating rate of 1000 K/s, the curve fit shown in Figure 16 b) is obtained. The volatile yields at 600 ° and 80 °C are constant when the residence time is 2 s or higher. Values with a volatile yield that is more than 10% higher than the mean value at 10 s are considered physically impossible and therefore neglected. At 1000 °C, the volatile yield is constant at all residence times. This means that the devolatilization is completed after a residence time of 2s at temperatures of 600 °C and 800 °C and after 1 s at a temperature of 1000 °C.

4.3.2. Release of Heavy Metals during Devolatilization in WMR

The release of heavy metals during pyrolysis is measured in this work by measuring their content in the char residues at discrete measuring points after devolatilization in the WMR. The release of the volatile elements Cd, Pb, and Zn is proportional to the temperature. Around 40% of the Pb is released at 60 °C (0% in the case of inert pyrolyzed sorghum) and around 95% at 1200 °C. While less than 20% of the Zn are released at 600 °C, more than 80% are released at 1200 °C. The different biomasses show the same behavior for the release of Zn and, except for inert pyrolyzed sorghum where the release is delayed, for Pb. For Cd, the deviation of the different biomasses is bigger at lower temperatures. While 78% of the Cd in the torrefied sorghum are released at 600 °C, 0% are released from the inert pyrolyzed sorghum. At higher temperatures, all the Cd is released. Non-volatile elements are enriched in the char residue and no substantial release is observed. This can, for example, be seen for Cu, which is below the detection limit before WMR experiments, while its concentration in the residues is between 10 mg/kg and 69 mg/kg. The release of Mn is always around 0%. Some Ti is released but does not show any temperature dependence and is likely only due to the high heating rate and Ti concentration in the biomasses. However, Fe, Cr, and Ni cannot be measured with this method because the wire mesh material (stainless steel) contains those metals which are therefore enriched in the residue by abrasion of the mesh material.

4.4. Release of Heavy Metals during Gasification in BabiTER

The BabiTER test rig at the TUM-CES is used for gasification experiments with torrefied, inert pyrolyzed, and oxidative pyrolyzed sorghum. As described in Section 2.3, the release of heavy metals during EFG is measured by measuring their content in solid samples that are withdrawn from the reaction zone with a sampling probe.

The release of Pb and Zn occurs in the investigated temperature range. Pb is the only one of the volatile heavy metals where the different biomasses show significant deviations to each other. While just below 30% of the Pb for the inert pyrolyzed sorghum and around 56% for the oxidative pyrolyzed sorghum are released at temperatures of 800 °C and 900 °C, more than 50% is released at temperatures of 1000 °C and above in the case of inert pyrolyzed sorghum and more than 75% in the case of oxidative pyrolyzed sorghum. Around 55% of the Pb is released at a temperature of 1100 °C in the case of torrefied sorghum from TNO. For all investigated sorghum samples, less than 10% of the Zn is released at temperatures of

800 °C and 900 °C, while between 30% and 45% are released at temperatures of 1000 °C and 1100 °C. Cd seems to be volatilized entirely in the investigated temperature range and the values below 100% lie within the inaccuracy of the measurement, especially in the ICP-OES due to the very low concentrations of Cd. Non-volatile elements are enriched in the solid samples and no substantial release is observed for Cu, Cr, Fe, Ni, and Ti, while some Mn is released in the case of torrefied and inert pyrolyzed sorghum.

4.5. Results Comparison and Summary

The combination of the WMR and the BabiTER experimental trials provides valuable insights into the various gasification processes involved in the conversion of sorghum in EFG. For torrefied sorghum, devolatilization increases notably from 600 °C to 800 °C, with complete release of volatiles occurring at 800 °C due to the significant volatile content of torrefied sorghum at 57wt.%$_{daf}$. The decomposition of cellulose and hemicellulose, occurring between 350 °C and 450 °C, leads to a substantial increase in volatile yield within the temperature range of 400 °C to 800 °C. Conversely, pyrolyzed sorghum exhibits a lower volatile content of only 12wt. %$_{daf}$, suggesting devolatilization during pretreatment, possibly influenced by the rapid heating rate. An increase in volatile yield is observed at temperatures of 1200 °C across all biomasses, particularly pronounced for pyrolyzed sorghum, indicating potential activation of chemical bonds within the pretreated biomass structure. However, the underlying mechanisms of this behaviour are complex and cannot be accurately predicted using first-order reaction kinetics-based models.

In BabiTER experiments, conversion rates of torrefied sorghum at 1100 °C are calculated to be 62% and 63% in two test campaigns, suggesting near-complete conversion of carbon to CO. In the gasification of inert pyrolyzed sorghum, conversions range between 21% at 800 °C and 33% at 1100 °C, while oxidative pyrolyzed sorghum yields conversions between 26% at 900 °C (29% at 800 °C) and 37% at 1100 °C. Notably, conversions of pyrolyzed sorghum are lower compared to torrefied sorghum due to differences in volatile and ash content. Conversion rates increase with temperature, indicating incomplete conversion at lower temperatures, potentially attributed to the formation of carbon dioxide and subsequent oxygen uptake by carbon atoms.

Regarding the release of volatile heavy metals (Pb, Cd, Zn), experimental results from various methods demonstrate good agreement. For Pb, torrefied and oxidative pyrolyzed sorghum exhibit consistent release behavior, while inert pyrolyzed sorghum shows faster volatilization in the ETV compared to other methods. However, there is no significant difference in Pb release among different biomass types in the ETV, suggesting minimal influence of pretreatment on Pb release. Cd release occurs predominantly between 500 °C and 600 °C, with slower release observed in pyrolyzed sorghum due to changes in the chemical environment during pretreatment. In the BabiTER, Cd volatilization appears to be promoted by exothermic reactions in oxidative conditions, while background noise may affect measurement accuracy at lower concentrations. Zn release is observed mainly between 900 °C and 1200 °C, with some volatilization at lower temperatures possibly influenced by the reducing atmosphere. Slower release of Zn between 1100 °C and 1500 °C is attributed to the formation of stable compounds.

In summary, the experimental results obtained with the different methods show good agreement with each other and therefore validate each other. While the overall release behavior is the same for all methods, the volatilization tends to occur at slightly higher temperatures in the BabiTER. The mass fraction of the heavy elements in the gas phase is especially lower at high temperatures (1100 °C). This is likely due to the more oxidizing atmosphere in the BabiTER. The volatilization of Cd and Zn is restrained in an oxidizing atmosphere because, in the presence of oxygen, their oxides are formed. Cadmium oxide (CdO) and zinc oxide (ZnO) have much higher boiling points than Cd and Zn in elemental form. Usually, a more oxidative atmosphere promotes the volatilization of Pb, but the opposite effect can arise when Pb is bound in metal-matrix complexes.

5. Conclusions and further steps

The GOLD project's Biomass-to-Liquid process presents an economically and environmentally promising approach to combe the two targets of recovering contaminated land for agricultural use while producing clean and sustainable biofuels with little indirect land use change (ILUC) from high-yield lignocellulosic plants. The produced biomass from contaminated land (WP1) is thermochemically converted into syngas via high-temperature entrained-flow gasification as investigated at the TUM Chair of Energy Systems (TUM-CES). After gas cleaning, the produced syngas can be fermented to ethanol and higher alcohols while heavy metals and metalloid contaminants are preferably removed in the non-leachable, vitrified slag.

Syngas composition (O_2, N_2, CO, H_2, CO_2, CH_4) is crucial for syngas fermentation, which requires an O_2-free feed gas. N_2 and O_2 in syngas come from dosing, purging, and safety valves, not gasification itself. For high CO_2 and H_2 conversion, the H_2/CO_2 ratio before fermentation should approach 2 for acetate and 3 for ethanol. Since high CO_2 in syngas from entrained flow gasification is due to low product gas temperature and poor reactor design, an industrial gasification reactor would yield almost CO_2-free syngas. Estimating industrial-scale syngas compositions and closing the mass balance for C, H, N, S from biomass-to-syngas uses a thermodynamic model. Scaling the EFG to 10 MW_{th} at 1400 °C results in a syngas composition free of CO_2 and O_2, with a H_2/CO ratio of about 0.5 for torrefied and torwashed sorghum, and about 0.25 for pyrolyzed sorghum.

The TUM-CES process model in the GOLD project aims to evaluate equipment interaction and optimize overall process design, considering experimental results. A base case model was designed, featuring internal syngas recycle for fermentation, with H_2 and CO_2 separated via PSA before synthesis. The model was optimized for liquid product and energy yield, carbon efficiency, and energy efficiency. Despite nearly complete CO conversion, carbon efficiency is limited to 29% due to unconverted CO_2. The optimized model increases carbon efficiency to 40%, with an overall product yield of 0.35 $t_{product}/t_{biomass,dry}$, mostly ethanol, and improved biofuel energy yield. Energy efficiency is about 28%, with 44% of initial biomass energy lost.

Experimental results from different methods corroborate each other and validate the observed release behavior of volatile heavy metals. While overall release patterns are consistent across methods, slightly higher volatilization temperatures are observed in the BabiTER, likely due to its more oxidizing atmosphere. The lower mass fraction of heavy elements in the gas phase at high temperatures (1100 °C) can be attributed to the oxidizing conditions, which restrain Cd and Zn volatilization by forming their respective oxides. Additionally, the release behavior of Pb may be influenced by its binding in metal-matrix complexes. The main advantages of the employed ETV-ICP-OES system include a wide range of detectable elements, rapid analysis, little sample amounts, and little sample preparation. However, extensive calibration and validation efforts are necessary. Short measurement times due to the simultaneous measurement of multiple elements at the same time, high versatility and productivity, and a large working range make ICP-OES an established and widespread technique for elemental analysis. Therefore, the ETV is chosen as the standard method for the measurement of the release behavior of heavy metals from contaminated biomasses.

6. References

[Arena, 2012] Arena, Umberto: Process and technological aspects of municipal solid waste gasification. A review. In: Waste management 32 (2012), Nr. 4, S. 625–639.

[Baxter 1993] Baxter, Larry L.: Ash deposition during biomass and coal combustion: A mechanistic approach. In: Biomass and Bioenergy 4 (1993), Nr. 2, p. 85–102. – ISSN 09619534.

[Briesemeister et al., 2017] Briesemeister, L.; Kremling, M.; Fendt, S.; Spliethoff, H.: Air-Blown Entrained-Flow Gasification of Biomass: Influence of Operating Conditions on Tar Generation. In: Energy & Fuels, 2017. Doi:10.1021/acs.energyfuels.7b01801

[Cui etal. 2018] Cui, Xiaoqiang ; Shen, Ye ; Yang, Qianying ; Kawi, Sibudjing ; He, Zhenli ; Yang, Xiaoe ; Wang, Chi-Hwa: Simultaneous syngas and biochar production during heavy metal separation from Cd/Zn hyperaccumulator (Sedum alfredii) by gasification. In: Chemical Engineering Journal 347 (2018), p. 543–551. – URL https://www.sciencedirect.com/science/article/pii/S138589471830706X. – ISSN 1385-8947.

[Doll 2018] Doll, Kathrin ; Rückel, Anton ; Kämpf, Peter ; Wende, Maximilian; Weuster-Botz, Dirk: Two stirred-tank bioreactors in series enable continuous production of alcohols from carbon monoxide with Clostridium carboxidivorans. In: Bioprocess and biosystems engineering 41 (2018), Nr. 10, S. 1403–1416.

[Dossow et al., 2021] Dossow, M.; Dieterich, V.; Hanel, A.; Fendt, S.; Spliethoff, H.: Improving carbon efficiency for an advanced Biomass-to-Liquid process using hydrogen and oxygen from electrolysis. Renewable and Sustainable Energy Reviews 152, 2021, 111670

[Dossow etl al. 2023] Dossow, M.; Leuter, P.; Spliethoff, H. Fendt, S.: Process Modelling of Biofuel Production from Contaminated Biomass Through Entrained Flow Gasification and Syngas Fermentation. At 31st European Biomass Conference & Exhibition, in Bologna, Italy, 5th June 2023.

[Geißler, 2020] Dissertation Geißler, Andreas: Untersuchung des Reaktionsverhaltens von Reinbrennstoffen und Brennstoffmischungen bei der Flugstromvergasung, 2020. ISBN: 9783843945073

[Han and Levenspiel 1988] Keehyun Han, Octave Levenspiel: Extended monod kinetics for substrate, product, and cell inhibition, in: Biotechnology and Bioengineering, 1988 https://doi.org/10.1002/bit.260320404

[Higman & Van der Burgt, 2008] Higman, Chris and {van der Burgt}, Maarten: Gasification, 2. ed, 2008, ISBN: 9780750685283.

[Jiang etal., 2016] Jiang, Ying ; Ameh, Abiba ; Lei,Mei ; Duan, Lunbo ; Longhurst, Philip: Solid-gaseous phase transformation of elemental contaminants during the gasification of biomass. In: The Science of the total environment 563-564 (2016), p. 724–730.

[Kaltschmitt & Hartmann, 2009] Kaltschmitt, Martin and Hartmann, Hans and Hofbauer: Energie aus Biomasse: Grundlagen, Techniken und Verfahren}}, 2., neu bearb. und erw. Aufl., Springer, 2009 url = http://site.ebrary.com/lib/alltitles/docDetail.action?docID=10310211, isbn = 9783540850946, doi = 10.1007/978-3-540-85095-3

[Levenspiel 1980] Octave Levenspiel: The monod equation: A revisit and a generalization to product inhibition situations, in: Biotechnology and Bioengineering, 1980. https://doi.org/10.1002/bit.260220810

[Linak and Wendt 1994] Linak, William P. ; Wendt, Jost O.: Trace metal transformation mechanisms during coal combustion. In: Fuel Processing Technology 39 (1994), Nr. 1-3, p. 173–198. – ISSN 0378-3820.

[Manouchehrinejad et al., 2018] Manouchehrinejad, Maryam ; van Giesen, Ian ; Mani, Sudhagar: Grindability of torrefied wood chips and wood pellets. In: Fuel Processing Technology 182 (2018), p. 45–55.

[Meyer et al. 2016] Hans-Peter Meyer, Wolfgang Minas, Diego Schmidhalter: Industrial-Scale Fermentation, in Industrial Biotechnology: Products and Processes, 2016. https://doi.org/10.1002/9783527807833.ch1

[Mörtenkötter et al., 2024] Mörtenkötter, H.; Heilmeier, C.; de Riese, T.; Fendt, S.; Spliethoff, H.: Temperature resolved release of inorganic compounds from biomass, in Fuel 2024. Doi: 10.1016/j.fuel.2023.129939

[Netter et al. 2021] Netter, Tobias; Fendt, Sebastian; Spliethoff, Hartmut: A collection of model parameters describing the gasification behavior of different fuels under entrained flow conditions. In: Fuel, 2021. Doi: 10.1016/j.fuel.2021.120536

[Nocquet et al. 2014] Nocquet, Timothée ; Dupont, Capucine ; Commandre, Jean-Michel ; Grateau, Maguelone ; Thiery, Sébastien ; Salvador, Sylvain: Volatile species release during torrefaction of wood and its macromolecular constituents: Part 1 – Experimental study. In: 0360-5442 72 (2014), p. 180–187.

[Obernberger etal. (1997)] Obernberger, Ingwald ; Biedermann, Friedrich ; Widmann, Walter ; Riedl, Rudolf: Concentrations of inorganic elements in biomass fuels and recovery in the different ash fractions. In: Biomass and Bioenergy 12 (1997), Nr. 3, p. 211–224. – ISSN 09619534.

[Panagos etal. 2013] Panagos, Panos ; van Liedekerke,Marc ; Yigini, Yusuf ; Montanarella, Luca ; Martin-Olmedo, Piedad: Contaminated Sites in Europe: Review of the Current Situation Based on Data Collected through a European Network. In: Journal of Environmental and Public Health 2013 (2013), p. 158764. – ISSN 1687-9805.

[Prins et al. 2006] Prins, Mark J. ; Ptasinski, Krzysztof J. ; Janssen, Frans J.: More efficient biomass gasification via torrefaction. In: 0360-5442 31 (2006), Nr. 15, p. 3458–3470.

[Relvas et al., 2018] Relvas, Frederico and Whitley, Roger D. and Silva, Carlos and Mendes, Adrlio: Single-Stage Pressure Swing Adsorption for Producing Fuel Cell Grade Hydrogen, in Industrial & Engineering Chemistry Research, 2018. Doi = 10.1021/acs.iecr.7b05410.

[Riboldi and Bolland 2017] Riboldi, Luca and Bolland, Olav: Overview on Pressure Swing Adsorption (PSA) as CO2 Capture Technology: State-of-the-Art, Limits and Potentials, in Development of Integrated High Temperature and Low Temperature Fischer-Tropsch System for High Value Chemicals Coproduction, 2017. Doi = 10.1016/j.egypro.2017.03.1385.

[Ritz etl al. 2023] Ritz, M.; Dossow, M.; Spliethoff, H. Fendt, S.: Investigation of the Release Behavior of Heavy Metals during Gasification of Contaminated Biomass. At 31st European Biomass Conference & Exhibition, in Bologna, Italy, 6th June 2023.

[Rückel et. al., 2021] Rückel, Anton ; Hannemann, Jens ; Maierhofer, Carolin ; Fuchs, Alexander ; Weuster-Botz, Dirk: Studies on Syngas Fermentation With Clostridium carboxidivorans in Stirred-Tank Reactors With Defined Gas Impurities. In: Frontiers in microbiology 12 (2021), S. 655390.

[Rückel et al., 2022] Rückel, Anton and Oppelt, Anne and Leuter, Philipp and Johne, Philipp and Fendt, Sebastian and Weuster-Botz, Dirk: Conversion of Syngas from Entrained Flow Gasification of Biogenic

Residues with Clostridium carboxidivorans and Clostridium autoethanogenum, 2022 in Fermentation, url = https://www.mdpi.com/2311-5637/8/9/465, doi = 10.3390/fermentation8090465.

[Steibel, 2018,] Dissertation Steibel, Markus: Experimentelle Untersuchung der Flugstromvergasung von Festbrennstoffen bei hohen Drücken und hohen Temperaturen, 2018. ISBN: 978-3-8439-3677-4

[van Ginneken etal. 2007] van Ginneken, Luc ; Meers, Erik ; Guisson, Ruben ; Ruttens, Ann ; Elst,Kathy ; Tack, Filip M. G. ; Vangronsveld, Jaco ; Diels, Ludo ; Dejonghe, Winnie: phytoremediation for heavy metal–contaminated soils combined with bioenergy production. in: journal of environmental engineering and landscape management 15 (2007), Nr. 4, p. 227–236. – ISSN 1648-6897.

[Vervaeke etal. 2006] Vervaeke, P. ; Tack, F.M.G. ; Navez, F. ; Martin, J.; Verloo, M. G. ; Lust, N.: Fate of heavy metals during fixed bed downdraft gasification of willow wood harvested from contaminated sites. In: Biomass and Bioenergy 30 (2006), Nr. 1, p. 58–65. – ISSN 09619534.

[Xu et al.., 2011] Xu, Deshun ; Tree, Douglas R. ; Lewis, Randy S.: The effects of syngas impurities on syngas fermentation to liquid fuels. In: Biomass and Bioenergy 35 (2011), Nr. 7, S. 2690–2696.